Photon Factory Activity Report 2001 #19B
–Users' Report–

63 Local structures in graphite-like carbon oxide
Iwao SHIMOYAMA, Tetsuhiro SEKIGUCHI, Yuji BABA
11A,27A/2001G107

64 X-ray induced polymerization of Si resin and reduction of Pt catalysts
Kiyotaka ASAKURA, Mamoru TACHIKAWA
9A/2001G117

65 Structural change of REE coprecipitated with Fe-Mn oxyhydroxides
Atsuyuki OHTA, Hiroshi TSUNO, Hiroyuki KAGI, Yoshio TAKAHASHI, Masaharu NOMURA, Iwao KAWABE
12C/2001G122

66 Characterization of iron in airborne particulate matter by XANES technique
Motohiro HIRABAYASHI, Motoyuki MATSUO, Kiyoshi TANABE, Masaharu NOMURA
12C/2001G131

67 Local structure analysis of zeolite-supported Ni and Co sulfide catalysts possessing a high HDS activity by means of X-ray absorption spectroscopy
Takeshi KUBOTA, Yasuaki OKAMOTO
10B/2001G138

68 Local structure analysis of supported Co-Mo binary sulfide catalysts prepared by a CVD method by means of X-ray absorption spectroscopy
Takeshi KUBOTA, Takao KAWABATA, Keiji OCHIAI, Yasuaki OKAMOTO
10B,12C/2001G139

69 Structural study of zirconium in aqueous solution for transactinide element research
Kazuaki TSUKADA, Hiromitsu HABA, Masato ASAI, Kazuhiko AKIYAMA, Tsuyoshi YAITA, Hirokazu NARITA, Atsushi TOYOSHIMA, Ichiro NISHINAKA, Yuichiro NAGAME
27B/2001G140

70 Photo-induced magnetized state of Co(DTBSQ)(DTBCat)(phen)·$C_6H_5CH_3$ studied by X-ray absorption spectroscopy
Toshihiko YOKOYAMA, Kaoru OKAMOTO, Kensuke NAGAI, Toshiaki OHTA, Shinya HAYAMI, Zhong-Ze GU, Rie NAKAJIMA, Osamu SATO
9A,10B,12C/2001G141

71 Local structure analysis of metal sulfide catalysts for HDS by means of in situ fluorescence X-ray absorption spectroscopy
Takeshi KUBOTA, Naoto HOSOMI, Takashi MATSUI, Kyoko BANDO, Yasuaki OKAMOTO
9A/2001G303

72 Structure of low concentrations of vanadium supported on titania determined by X-ray absorption fine structure combined with fluorescence spectrometry
Yasuo IZUMI, Fumitaka KIYOTAKI, Ken-ichi AIKA, Hideaki YOSHITAKE, Tae SUGIHARA, Takashi TATSUMI, Yasuhiro TANIZAWA, Takafumi SHIDO, Yasuhiro IWASAWA
7C/2001G308

73 Structure of new rhodium catalysts prepared by surface molecular imprinting method
Mizuki TADA, Takehiko SASAKI, Takafumi SHIDO, Yasuhiro IWASAWA
10B/2001G315

74 In situ time-resolved energy-dispersive XAFS study on the structural changes of Rh/Al_2O_3 during CO adsorption and desorption
Akane SUZUKI, Aritomo YAMAGUCHI, Teiji CHIHARA, Yasuhiro INADA, Takafumi SHIDO, Kiyotaka ASAKURA, Masahiko ABE, Makoto YUASA, Masaharu NOMURA, Yasuhiro IWASAWA
10B,9C/2001G316

75 Chemical mapping of individual fluid inclusion by synchrotron X-ray fluoresence microprobe
Ken-ichiro HAYASHI, Hiroki NAGASEKI, Atsuo IIDA
4A/2001P004

76 Carbon K-edge NEXAFS study of carbonaceous matter in the Allende (CV3) carbonaceous chondrite
Fumio KITAJIMA, Kazuhiko MASE, Tomoki NAKAMURA, Eiichi KOBAYASHI, Kouji ISARI, Yoshinori KITAJIMA
8A,13C/2001P005

- *Crystallography*
- *Electronic Structure of Condensed Matter*
- *High Pressure Science*
- *Instrumentation and Technique*
- *Medical Applications*
- *Materials Science*
- *Surface and Interface*

7A,11A/1999G246

Site-specific ion desorption of methyl ester-terminated self-assembled monolayer (SAM) induced by core excitation

Erika O. SAKO, Ryohei SUMII, Satoshi WAKI,
Shin-ichi WADA, Tetsuji SEKITANI*, Kenichiro TANAKA
Hiroshima University, Higashi-Hiroshima, 739-8526, Japan

Introduction

Site-specific bond scission following core excitation has been studied for the aim of controlling chemical reactions. It was found that poly-methylmethacrylate (PMMA) thin film indicates remarkable site-specificity in the photon stimulated ion desorption (PSID) [1]. Self-assembled monolayer (SAM) is expected to be useful to get direct information about the effect of the functional group and molecular environment to the PSID reaction; because it is close-packed structure with the headgroup of adsorbate covalently bonds to a substrate and the terminated functional group are aligned on the topmost surface. In this study, the PSID reactions following core-excitation have investigated using the SAM of methyl 16-mercapto hexadecanate (MHDA: $HS-(CH_2)_{15}-COOCH_3$) on gold.

Experiment

The experiments were performed at the soft X-ray beamline BL-7A and 11A of the Photon Factory (KEK-PF). Total electron yield (TEY) spectra were obtained by measuring the sample drain-current. Desorbed ions were detected using a time-of-flight mass spectrometer (TOF-MS) combined with pulsed SR (single bunch mode) at an angle of 60° with respect to the SR beam (30° from to the sample surface). Total ion yield (TIY) spectra were measured by detecting non-select ions. In the measurement of the desorbed ions, the sample surface is located at the normal direction and 12~15 mm away from the TOF-MS.

Results and Discussion

In the TEY spectrum, the absorption for methyl ester group is similarly observed with PMMA and for methylene chain is observed with typical alkanethiol SAM. The ion desorption efficiency (IDE) which obtained by dividing TIY by TEY, was enhanced at 289.4 eV, C 1s $\rightarrow$ σ^* ($O-CH_3$) excitation. Similar enhancement was observed for PMMA, but the enhancement of the MHDA is larger than PMMA. Fig. 1 show the partial ion yield (PIY) spectra of typical ions, H^+, CH_n^+ (n=1, 2, 3), $C_2H_3^+$, and $C_2H_5^+$ together with the TEY spectrum of MHDA in the carbon core excitation region. From this figure, CH_n^+ (n=1, 2, 3) ions are observed selectively at the resonant transition of C 1s to σ^* ($O-CH_3$) orbital. The spectra of other ions do not have such a specific feature.

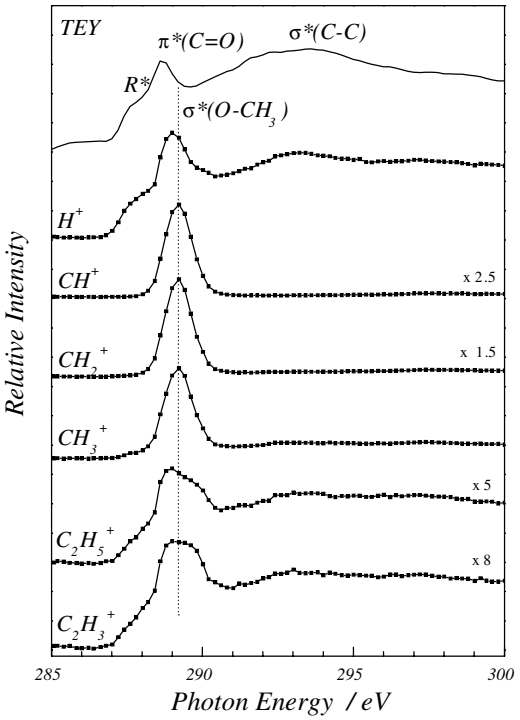

Fig. 1. TEY and PIY spectra of H^+, CH_n^+ (n=1-3), $C_2H_3^+$ and $C_2H_5^+$ of MHDA in the C K-edge

For example, the PIY spectrum of H^+ ion follow the features of the TEY spectrum, therefore the indirect photo desorption is dominant mechanism in the H^+ desorption.

The site-specificy of CH_3^+ ions are more clear than that of PMMA in the point of the decrease of the ion yields of indirect reaction. These results indicate that the molecular environment affect strongly the site-specific reaction.

References

[1] K. Tanaka *et al.*, J. Electron Spectrosc. Relat. Phenom. 119, 255 (2001).

* sekitani@sci.hiroshima-u.ac.jp

10B/99G253

XAFS study on structure of Bi species supported on amorphous silica

Chizu MURATA, Tomoaki SUNADA, Hisao YOSHIDA*, Tadashi HATTORI
Department of Applied Chemistry, Graduate School of Engineering,
Nagoya University, Nagoya 464-8603, Japan

Introduction

The direct gas phase epoxidation of propene by molecular oxygen has been desired, and has been attempted by many researchers. As a new approach, we have investigated 'photoepoxidation' of propene using only O_2 over several systems, and have reported that Bi_2O_3/SiO_2 showed high activity for propene photoepoxidation [1]. In the present study, we prepared a series of Bi_2O_3/SiO_2 samples, and investigated the structure of Bi species on silica and their propene photoepoxidation activity.

Experimental

Bi_2O_3/SiO_2 was prepared by the conventional impregnation method from amorphous silica prepared by sol-gel method with a nitric acid aqueous solution of $Bi(NO_3)_3$, followed by calcination at 773 K for 5 h in flowing dried air. The photooxidation of propene was performed in a similar manner as previously reported. [1]

Bi L_{III}-edge XAFS spectra were measured at the BL-10B station [2] at KEK-PF with a Si(311) channel cut monochrometer in transmission mode at room temperature. Prior to measurement, the samples were treated with 100 Torr oxygen (1 Torr = 133.3 N m^{-2}) at 773 K for 1 h, followed by evacuation at 673 K for 1 h. The pretreated sample was sealed in a polyethylene bag under a dried N_2 atmosphere without exposing to air.

Results and Discussion

The photooxidation of propene by molecular oxygen was investigated over Bi_2O_3/SiO_2 samples containing different amount of Bi (0.7 – 30 mol%). With increasing Bi content, the conversion of propene increased up to 1.5 mol% of Bi, and then decreased. The selectivity to PO was high such as 23 % on the samples containing below 1.5 mol% of Bi, and decreased with increasing Bi content. These results mean that the highly dispersed Bi species would be active sites for this reaction.

From XRD patterns, it was shown that α-Bi_2O_3, β-Bi_2O_3 and Bi_2SiO_5 were formed over the Bi_2O_3/SiO_2 samples containing more than 10 mol% of Bi.

Fig. 1 shows the Fourier Transforms of Bi L_{III}-edge EXAFS spectra of Bi_2O_3/SiO_2 and Bi_2O_3 samples. All of Bi_2O_3/SiO_2 samples showed a clear maximum at 1.65 Å owing to Bi-O bonds. Bi_2O_3/SiO_2 0.7 mol% and 1.5 mol% samples showed the peak with high intensity. With increasing Bi content, the peak became lower. This would be attributed to the formation of α-Bi_2O_3, β-Bi_2O_3 and Bi_2SiO_5 that have a variety of Bi-O distances. The peaks due to Bi-Bi bonds were not clearly observed over all the spectra of Bi_2O_3/SiO_2 samples.

Table 1 shows structural parameters of the first Bi-O shell determined by the curve-fitting analysis on Fourier-filtered EXAFS of Bi_2O_3/SiO_2 0.7 mol% and 1.5 mol % samples using empirical parameters of Pb-O shell extracted from EXAFS spectrum of PbO. $\Delta(\sigma^2)$ corresponds to the relative Debye-Waller factor deviated from those of PbO (Pb-O shell). The coordination number and the distance of the nearest Bi-O bond were 4.0 ± 0.1 and 2.31 Å, respectively. This coordination number is quite different from those of α-Bi_2O_3, β-Bi_2O_3 and Bi_2SiO_5. Bi species would be highly dispersed and 4-fold coordinated in the silica matrix below 1.5 mol% of Bi content.

From these results, it is suggested that the highly dispersed tetrahedral Bi species are active for photoepoxidation of propene, while the Bi clusters, α-Bi_2O_3, β-Bi_2O_3 and Bi_2SiO_5, are less active for photooxidation of propene.

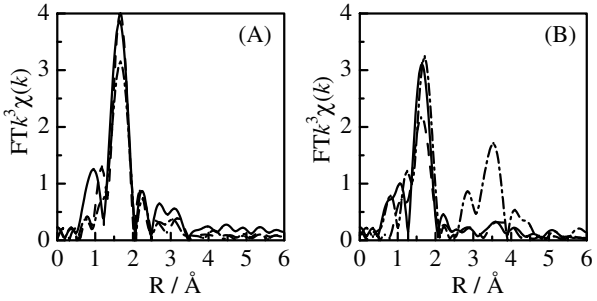

Fig. 1 Fourier Transforms of Bi L_{III}-edge EXAFS spectra of (A) Bi_2O_3/SiO_2 0.7 mol % (——), 1.5 mol % (- - -), and 3.0 mol % (—·—). (B) Bi_2O_3/SiO_2 10 mol % (——), 30 mol % (- - -), and Bi_2O_3 (—·—). The *k*-range for the Fourier transformation: 4-12 $Å^{-1}$.

Table 1 Curve-fitting results on Fourier-filtered EXAFS of Bi_2O_3/SiO_2 samples.

Bi content / mol %	CN	r / Å	$\Delta(\sigma^2)$ / 10^{-3} $Å^2$	R_f /%
0.7	4.1	2.31	-3.41	10.5
1.5	3.9	2.31	-3.31	9.65

The *R*-range for back Fourier transformation: 1.1-2.3 Å, the curve fitting *k*-range : 4-11$Å^{-1}$.

References

[1] H. Yoshida, et al., J. Catal., **194**, 364 (2000).
[2] M. Nomura et al., KEK Report 89-16, (1989).

* yoshidah@apchem.nagoya-u.ac.jp

9A/1999G257

Vertical distribution of iron species in sediments from Qinghai Lake, China

Akihito KUNO*, Motoyuki MATSUO
The Univ. of Tokyo, Komaba, Meguro-ku, Tokyo 153-8902, Japan

Introduction

Qinghai Lake is the largest salt lake in China. Although a number of investigations have been carried out on marine and coastal sediments, there have been few studies on iron speciation of lacustrine sediments, especially sediments collected from salt lakes. In marine and coastal sediments, sulfate ion from seawater is reduced to hydrogen sulfide, which reacts with iron compounds to form iron sulfides. Therefore, the speciation of iron compounds in the sediments collected from salt lakes, which also contain sulfate ion, receives much attention from geochemical point of view. In addition, Qinghai Lake sediments are intensively studied to reconstruct the past climate by carbonate content, fossil pigments, etc., since vertical sediment cores record the climatic change. Among such reconstruction studies, the iron speciation using XANES spectroscopy has the advantage of non-destructiveness and sensitivity to environmental change. From these standpoints, the iron speciation in the Qinghai Lake sediment was carried out using XANES spectroscopy in this study.

Experimental

Qinghai Lake, an intermontane plateau lake, lies on the northeastern edge of the Tibetan Plateau, near N37°, E100°, with an area of 4200 km^2. It has a surface elevation of 3194 m, an average depth of more than 20 m, pH value 9.21, density 1.01, and salinity 14.15 g/L. A vertical sediment core of approximately 350 cm in length was collected from southeastern part of Qinghai Lake. It is considered to record the environmental change during the past nine thousand years based on the estimated sedimentation rate (40 cm/ka). The collected sediment was cut at every 2-3 cm length, freeze-dried, and ground into powder. Approximately 200 mg of each sample was mounted in a sample holder. In order to avoid air oxidation, the sediments were purged with nitrogen gas in oxygen-impenetrable plastic bags. The Fe K-absorption spectra of the sediments were measured in fluorescence mode using a Si(111) double-crystal monochromator and a Lytle-type detector at BL-9A. The sediments were also analyzed by ^{57}Fe Mössbauer spectroscopy.

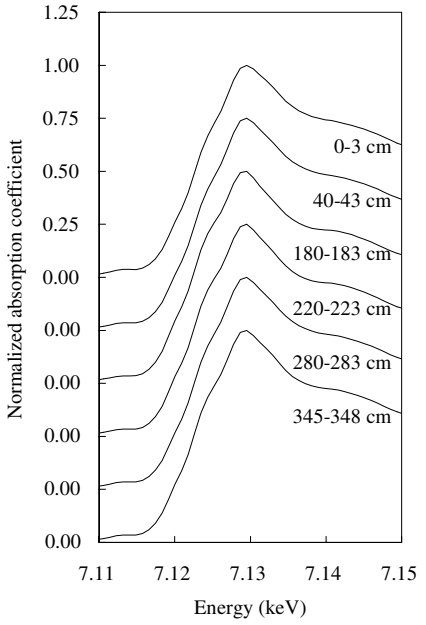

Fig. 1: Fe XANES spectra of the sediments collected from Qinghai Lake.

Results and discussion

Figure 1 shows a composite of six XANES spectra out of eighteen spectra of the sediments collected from different depths, in which slight shifts of the spectra were observed. Comparison with the speciation results by Mössbauer spectroscopy revealed that the shifts to a lower energy side were mainly due to the existence of pyrite (FeS_2). This is often the case with sediments under saline waters [1,2]. Also, framboidal pyrite particles were found in Qinghai Lake sediments by scanning electron microscope. The vertical distribution of pyrite showed a positive correlation with the organic matter content measured by the loss on ignition (LOI), which increases under warm climate. This observation is reasonable because one of the factors controlling sulfate reduction is temperature that strongly affects the activity of sulfate reducing bacteria. A high content of organic matter produces reducing environment, which also favors the activity of sulfate reducing bacteria. The distribution of pyrite and sedimentation rate suggested a relatively warmer climate around 500, 2500, 4500, and 7000 years B.P., which was consistent with other reconstruction studies [3].

References

[1] A. Kuno et al., J. Synchrotron Radiat. 6, 667 (1999).
[2] A. Kuno, Bunseki Kagaku 51, 287 (2002).
[3] A. Kuno et al., Hyperfine Interact. in press (2002).

* kuno@dolphin.c.u-tokyo.ac.jp

12C / 2000G071

Local structures of $RbMnFe(CN)_6$ studied by EXAFS: The photoinduced phase and the high- and low-temperature phases

Toshihiko YOKOYAMA[1]*, Hiroko TOKORO[2], Shinichi OHKOSHI[2], Kazuhito HASHIMOTO[2], Kaoru OKAMOTO[3] and Toshiaki OHTA[3]

[1]Institute for Molecular Science, Myodaiji-cho, Okazaki, Aichi 444-8585, Japan

[2] Res. Center for Adv. Science & Technol., The Univ. of Tokyo, Komaba, Tokyo 153-0041, Japan

[3]Dept. Chemistry, Graduate School of Science, The Univ. of Tokyo, Hongo, Tokyo 113-0033, Japan

Introduction

A Prussian-blue analogue of $RbMnFe(CN)_6$ shows a thermally induced first-order phase transition at T_c =231 K and T_c =304 K [1] and a photoinduced phase transition at very low temperature. Especially, below T_c=12 K, spontaneous magnetization is quenched rapidly by the visible-light irradiation.

In the present study, we have investigated the local structures in the low-temperature (LT), high-temperature (HT) and photo-induced (PI) phases of $RbMnFe(CN)_6$ by measuring Mn, Fe and Rb *K*-edge EXAFS.

Experimental

The Mn, Fe and Rb K-edge EXAFS spectra were recorded with a transmission or fluorescence-yield mode at BL12C at the temperatures of 300 K for the HT phase and 30 K for the LT and PI phases. The PI phase was obtained by irradiating the visible light (532 nm, Nd:YAG laser) at 30 K and the fluorescence-yield spectra were taken under irradiation.

Results and discussion

Figures 1 and 2 shows the Fourier transforms of Fe and Mn *K*-edge EXAFS, respectively, taken with the fluorescence-yield mode. In principle, three peaks are seen in both figures. In Fig. 1, the peaks at 1.5, 2.6 and 4.6-4.8 Å are ascribed to the Fe-C, Fe-N and Fe-Mn shells, respectively. Similarly, the Mn-N, Mn-C and Mn-Fe shells can be found in Fig. 2. Since the present material shows a NaCl-type framework, higher-nearest neighbor shells are enhanced due to the multiple-scattering focusing effect.

The curve-fitting analysis was performed assuming the collinear configuration of the –Fe-C-N-Mn- chain. The Fe-C distances were obtained as 1.914 0.003, 1.897 0.004 and 1.93 0.02 Å for the HT, LT and PI phases, respectively. The presence of the octahedral $Fe(CN)_6$ unit is clearly confirmed. These results indicate that Fe is in the divalent state in the LT phase and is in the trivalent state in the RT and PI phases.

Two kinds of the Mn-N distances of ~1.96 and ~2.21 Å were found in all the phases. The coordination number for each shell changes drastically, depending on the phases. The longer Mn-N bonds are dominated in the HT and PI phases, while both contributions are clearly seen in the LT phase. In the HT and PI phases, an octahedral $Mn(NC)_6$ unit is most probable with divalent high-spin d^5 Mn and with the longer Mn-N distance of ~2.21 Å. A small contribution from the shorter Mn-N bond in the HT and PI phases might be caused by the coexistence of the LT phase, this being confirmed by XANES.

In the LT phase, it is concluded that the $Mn(NC)_6$ unit is Jahn-Teller distorted, leading to four shorter and two longer Mn-N bonds. This is typical in trivalent high-spin Mn and the tetragonal distortion observed by powder x-ray diffraction is explained by the present findings. Moreover, the Mn-Fe and Fe-Mn distances agree excellently with those estimated from the lattice constants of the HT and LT phases. From the Rb *K*-edge EXAFS, Rb is found to locate at the center of the cubic framework.

The local structures of all the phases were successfully determined and the PI phase is found to be structurally identical to the HT phase.

References

[1] S. Ohkoshi et al., J. Phys. Chem. 106, 2423 (2002).

* yokoyama@ims.ac.jp

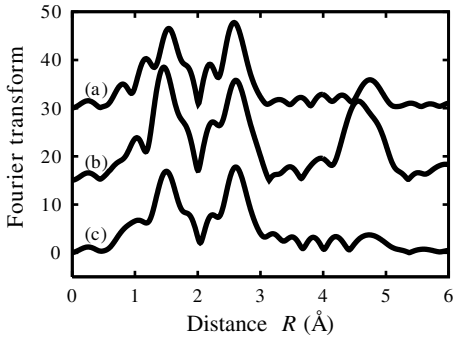

Fig. 1 Fourier transforms of Fe *K*-edge EXAFS of (a) the HT phase, (b) the LT phase and (c) the PI phase.

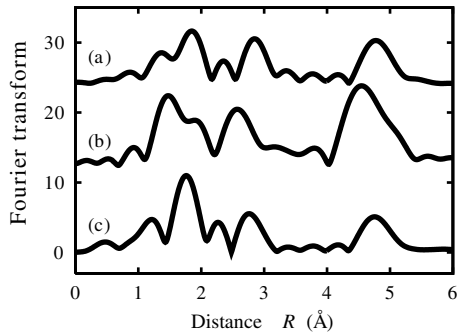

Fig. 2 Fourier transforms of Mn *K*-edge EXAFS of (a) the HT phase, (b) the LT phase and (c) the PI phase.

12C / 2000G071

Photoinduced phase transition of $RbMnFe(CN)_6$ studied by XANES

Toshihiko YOKOYAMA[1]*, Hiroko TOKORO[2], Shinichi OHKOSHI[2], Kazuhito HASHIMOTO[2], Kaoru OKAMOTO[3] and Toshiaki OHTA[3]

[1]Institute for Molecular Science, Myodaiji-cho, Okazaki, Aichi 444-8585, Japan

[2] Res. Center for Adv. Science & Technol., The Univ. of Tokyo, Komaba, Tokyo 153-0041, Japan

[3]Dept. Chemistry, Graduate School of Science, The Univ. of Tokyo, Hongo, Tokyo 113-0033, Japan

Introduction

Recently Ohkoshi et al. discovered a photoinduced (PI) phase transition in a Prussian-blue analogue of $RbMnFe(CN)_6$. $RbMnFe(CN)_6$ exhibits the magnetic phase transition at T_c=12 K, below which the material shows spontaneous magnetization. Upon visible-light irradiation (650 nm), the spontaneous magnetization is quenched completely, and some minutes after turning off the light the magnetization is recovered abruptly.

In the present study, we have investigated the electronic state in the PI phase of $RbMnFe(CN)_6$ by measuring Mn, Fe and Rb *K*-edge XANES.

Experimental

The Mn, Fe and Rb *K*-edge XANES spectra were recorded with a transmission or fluorescence-yield mode at BL12C at the temperatures of 300 K for the high-temperature (HT) phase and 30 K for the low-temperature (LT) and PI phases. The PI phase was obtained by irradiating the visible light (532 nm, Nd:YAG laser) at 30 K and the fluorescence-yield spectra were taken under irradiation.

Results and discussion

Figure 1 shows the preedge region of the Fe *K*-edge XANES. The sample in the dark gives a single absorption band indicated by an arrow in the 1*s* 3*d* transition. This band is split into two components when irradiated by the lights. The occurrence of the phase transition is clearly identified. The splitting is ascribed to the crystal-field splitting associated with the presence of the hole in the $3dt_{2g}$ level. These findings imply that Fe is in the low-spin (LS) trivalent (d^5) and LS divalent (d^6) states in the LT and PI phases, respectively. The PI phase seems identical to the HT one consisting of LS trivalent (d^5) Fe.

Figure 2 shows the preedge region of the Mn *K*-edge XANES. Although the spectral features in the 1*s* 3*d* transition regions is less clear, the spectrum in the dark gives double peaks, which is merged to a single peak under light irradiation. The spectrum of the PI phase is again similar to the HT one. By comparing the spectra in Fig. 2, we can conclude that the PI phase consists of high-spin (HS) divalent (d^5) Mn as in the case of the HT phase, while the LT phase gives high-spin trivalent (d^4) Mn.

Although the overall features of the Mn *K*-edge XANES are found to change drastically between the LT and PI phases and to be similar between the PI and HT phases, this cannot be shown due to the limitation of the report and will be given elsewhere. As a consequence, upon light irradiation, the charge-transfer tautomeric photoinduced transition takes place and the electronic state turns from Fe(II)LS-Mn(III)HS to Fe(III)LS-Mn(II)HS. The PI phase is identical to the HT phase.

* yokoyama@ims.ac.jp

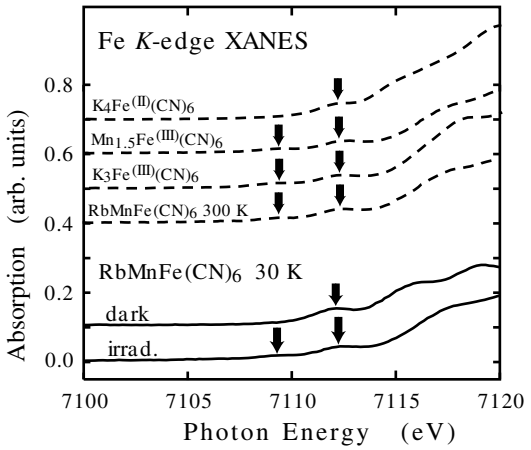

Fig. 1 Preedge region of the Fe *K*-edge XANES of the LT (dark) and PI (irrad.) phases, together with those of the HT phase (300 K) and other reference materials.

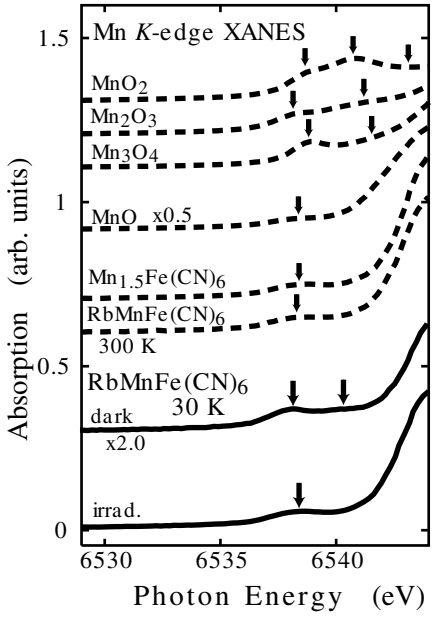

Fig. 2 Preedge region of the Mn *K*-edge XANES of the LT (dark) and PI (irrad.) phases, together with those of the HT phase (300 K) and other reference materials.

10C/2000G247

Structures of molecular assembly formed by sugar-based surfactants having branched alkyl chains in water

Itaru YAMASHITA[1], Tadashi KATO*[1], Hirohisa YOSHIDA[2],
Hiroyuki MINAMIKAWA[3], and Masakatsu HATO[3],
[1]Department of Chemistry, Tokyo Metropolitan University,
Hachioji, Tokyo 192-0397, Japan
[2]Department of Applied Chemistry, Tokyo Metropolitan University,
Hachioji, Tokyo 192-0397, Japan
[3]Nanotechnology Research Institute, AIST, Tsukuba, Ibaraki 305-8565, Japan

Introduction

In recent years, much attention has been paid to the sugar-based surfactants such as alkyl glucoside from the ecologial and industrial viewpoints. However, the Kraft temperature (T_K) of them is usually higher than room temperature, which seriously limits the usefulness of them in many technological applications and also make it difficult to study the strutures of micellar and liquid crystal phases. Recently, Hato et al. [1] have synthesized novel alkylglycoseds, that consist of an isoprenoid-type hydrophobic chain, the 3,7,11,15-tetramethylhexadecyl (phytanyl) group. It has been shown that T_K of these surfactants are significantly lower than room temperature and that they exhibit interesting phase behaviors. In the present study, we have measured small angle x-ray scattering on aqueous solutions of 1-*o*-*β*-3,7-dimethyoctyl-*D*-glucopyranoside (abbreviated as Glu(Ger)) as well as aqueous mixtures of Glu(Ger) and 1-*o*-*β*-3,7-dimethyoctyl-*D*-maltoside (Mal(Ger)). To investigate effects of branching of alkyl chains, the same measurements have been made for aqeuous solutions of 1-*o*-*β*-decyl-*D*-glucopyranoside (Glu(C10)) and 1-*o*-*β*-decyl-*D*-maltoside (Mal(C10).

Experimental

Measurements were performed using SAXS spectrometer installed at the BL-10C instrument at the Photon Factory of the National Laboratory. We used a sample cell made of copper with Kapton windows (sample thickness = 1mm) whose temperature is controlled by using the DTA/SAXS instrument reported before.

Analyses

Observed scattering intensity curves were analyzed by the following procedure. For monodispersed system of ellipsoidal micelles, the scattering intensity can be expressed as

$$I(q) = AN_p\left[\langle F(q)^2\rangle + \langle F(q)\rangle^2 (S(q)-1)\right] \quad (1)$$

where N_p is the number density of micelles, $F(q)$ is the single particle form factor, and $S(q)$ is the structure factor depending on intermicellar interactions. The form factor $F(q)$ can be expressed as:

$$\langle F(q)^2\rangle \equiv \int |F(q,x)|^2 dx \quad \langle F(q)\rangle^2 \equiv \left|\int F(q,x)dx\right|^2$$

$$F(q,x) = (B_C - B_S)V_C[3j(u_C)/u_C] + (B_S - B_W)V[3j(u)/u]$$

$$u_C \equiv qR_C\sqrt{x^2 + a_C{}^2(1-x)}$$

$$u \equiv qR\sqrt{x^2 + a^2(1-x)}$$

where B_c, B_s, and B_w are the scattering length densities of the micellar core, micellar shell including hydrated water, and solvent, respectively, j is the first order spherical Bessel function, R_c and R are the semiminor axes of the micellar core and whole micelle, respectively, V_c and V are volumes of the micellar core and whole micelle, respectively, and a_c and a are the axial ratios of the micellar core and whole micelle, respectively. All the parameters needed to calculate $I(q)$ are functions of R_c, a_c, and the thickness of the micellar shell, which are used as free-fitting parameters in the nonlinear least-squares analysis of the data. In addition to them, a scaling parameter, A, was used as a free-fitting parameter due to uncertainty in calibration for absolute intensity.

Results

First, we have analyzed the scattering intensity for single-component micelles formed by Mal(C10) or Mal(Ger) (5 % by weight at 30°C). The observed scattering curves can be fitted by prolate ellipsoid better than oblate ellipsoid. The obtained axial ratios of the micellar core are about 1.8 and 2.1 for Mal(C10) or Mal(Ger), respectively. The thickness of the micellar shell is about 1.0 nm for both micelles, as expected. Then the mole fraction of Glu(C10) and Glu(Ger) in the total mixed solute (the total weight concentration was fixed to 5wt%) is increased up to 0.9 and 0.55, respectively. As the mole fraction of glucoside increases, the axial ration increases up to about 2.5 for both systems.

References

[1] M. Hato, H. Minamikawa, R. A. Salkar, and S. Matsutani, Langmuir **18**, 3425 (2002).

* kato-tadashi@c.metro-u.ac.jp

9A/2000G262

In Situ XAFS investigation of iron hydrous oxide in alkaline solution

Sunghyun KIM*[1], Hyukjae CHOI[1], Jae-Woo KIM[2], Su-Moon PARK[2], Toshiaki OHTA[3]
[1]Department of Chemsitry, Konkuk University, Seoul 143-701, Korea
[2]Department of Chemistry, Pohang University of Science and Technology, Pohang 790-784, Korea
[3]Department of Chemistry, School of Science, The University of Tokyo, Tokyo 113-0033, Japan

Introduction

Transition metal oxides play an important role in the field such as batteries, electrochromic displays, and electrocatalysis. Thus the structural elucidation is of importance to understand the system better. The XAFS study has mostly been centred on the nickel (hydr)oxide and additives. For example, it is well known that cobalt improves the charge acceptance of the nickel electrode in alkaline media, thus offering higher battery performance [1]. The role and structural aspects of cobalt both in nickel hydroxide lattice and in pure cobalt hydroxide systems have been thoroughly studied as a function of the oxidation states of Ni and Co [2].

The study of iron (hydr)oxide system is technologically important in that it is closely related to corrosion process or Fe/Ni, Fe/air battery systems. Electrochemically iron undergoes quite complex redox state changes and phase transformations. It is rather surprising that while synthesis and chemical conversion between iron oxides have been well established, the structural behavior of iron oxides is poorly understood.

Experimental

All the experiments was carried out *in situ* in a fluorescence mode using a cell developed by Kim et al., where the carbon sheet can serve as a working electrode as well as a window. Iron hydrous oxide was deposited onto the carbon surface by passing -5 mA for 10 min through the ferric nitrate containing solution, which causes OH^- near the surface, leading to iron hydroxide precipitate on the electrode surface. Before the XAFS measurements, cyclic voltammetry was performed to confirm the electrochemical behaviour. Iron hydrous oxide exhibits two main redox peaks corresponding to Fe^{2+} and Fe^{3+} whose potential was separated by ca. 350 mV. Potential was fixed where iron existed as +2, +3. To get the intermediate oxidation states, potential was scanned from the +2 state to the rising position of a voltammogram and came back to the +2 state. For the identification of electrochemically prepared iron species, iron(II) and iron (III) (hydr)oxides were prepared by adding ammonia to the solution containing $FeSO_4$ and $Fe(NO_3)_3$, respectively.

Results and Discussion

FeOOH samples from our lab (curve a) and Aldrich (curve b) show almost identical XANES spectra (Figure 1). A distinct pre-edge peak at 7114.1 eV is the indication of 1s → 3d transition, showing the symmetry around Fe is not hexagonal but little distorted. The similar behavior has been observed for NiOOH. Iron(II) species shows very different XANES (curve c) in which a rather broad pre-edge peak appeared at 7112.8 eV and the edge position at $\mu = 0.5$ shifts considerably from 7123.2 eV to 7119.0 eV. The pre-edge shift approximately follows the rule that +1 oxidation change gives rise to ca. 1 eV. The absorption edge shift is usually much larger than that of a pre-edge. Notable is the highly increased white line intensity for iron(II) species, which is tentatively assigned as $Fe(OH)_2$. FT analysis shows d(Fe-O) at 1.474, and 1.572 Å for FeOOH (Aldrich) and $Fe(OH)_2$, respectively, showing the lattice contraction by oxidation.

Curves d to g are *in situ* XANES as a function of potential. The absorption edge gradually moves to the higher energy as the oxidation number increases. $E_{\mu=0.5}$ = 4.6 eV indicates that the whole iron (II) state was converted to iron (III) state. This is in contrast to the case of cobalt, where only part of cobalt spcies undergoes oxidation state change. There are at least two isosbestic points (7131.1 and 7178.5 eV), indicating that only two principal species exist.

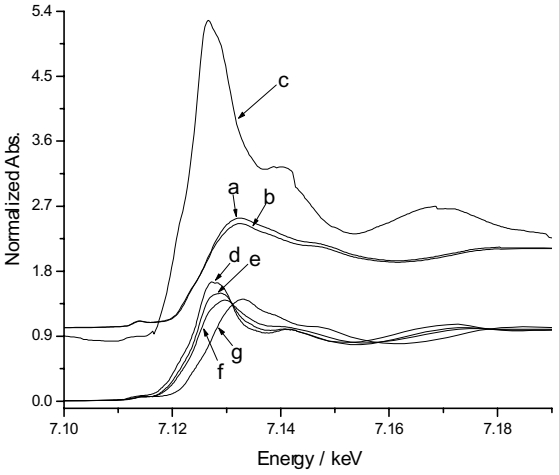

Figure 1. XANES spectra of FeOOH prepared in the lab (a) and from Aldrich (b), and $Fe(OH)_2$ (c). Curves d to g are *in situ* spectra obtained by sequentially polarizing the electrode from +2 (d) to +3 (g) state of iron.

References

[1] S. Kim et al., J. Phys. Chem. **98**, 10269 (1994).
[2] D. Totir et al. J. Electrochem. Soc. **147**, 4594 (2000).

* skim100@konkuk.ac.kr

9A/2000G263

Local structure of Ni hydroxide cluster synthesized by the microemulsion method

Kensuke NAGAI, Kaoru OKAMOTO, Jyun MIYAWAKI, Hiroshi KONDOH, Toshihiko YOKOYAMA, Toshiaki OHTA*
Department of Chemistry, Graduate School of Science, The University of Tokyo, 7-3-1 Hongo, Bunkyo-ku, Tokyo 113-0033, Japan

Introduction

Although metal compound clusters are expected to have unique physicochemical properties, they are often unstable under atmospheric condition. Recently, the microemulsion method has been developed, in which clusters are synthesized in micro-spaces inside inverse micelles and protected by surfactant molecules. The clusters are often self-assembled to form a super-lattice structure called 'nanocrystal'. Using this method, we synthesized Ni hydroxide clusters, and measured their magnetization by SQUID. Although the bulk sample of Ni hydroxide shows antiferromagnetism, the synthesized cluster shows a hysterisis curve in the field-dependent magnetization below 10K. This behavior is interpreted by super-paramagnetism; although spin's magnetic moment is oriented to one direction in each cluster, no magnetic interactions operate between them. In this work, we measured and analyzed Ni *K*-edge XAFS spectra of Ni hydroxide clusters, and from these results, we discussed the correlation between their structures and magnetic properties.

Experimental

Xylene solution of a surfactant (diisooctyl sodium sulfosuccinate (AOT)) were added to 0.1 mol/l $Ni(NO_3)_2$ aqueous solution. Then 0.1 mol/l KOH aqueous solution was poured into the solution and was stirred. Ni hydroxide clusters were obtained from an organic phase. In the microemulsion method, the cluster size is controlled by the molar ratio of a surfactant. These clusters are too small to measure the powder x-ray diffraction quantitatively. And they are so easily damaged by high-energy electron beam that TEM images could not be obtained. Ni *K*-edge XAFS spectra were measured at 16-18 K with the transmission mode at BL-9A using a Si(111) double-crystal monochromator. Sample powders were diluted by BN and pressed into disks.

Results and Discussion

Ni *K*-edge XANES of Ni hydroxide cluster are almost identical with that of the bulk compound, revealing that the electronic structure around Ni atoms does not change as the cluster size becomes smaller. Fig. 1 shows Fourier transforms of Ni *K*-edge EXAFS spectra, and Table 1 lists the interatomic distances obtained from the EXAFS analysis. The results indicate that the cluster's distances of Ni-O1 and Ni-Ni1 become shorter and the coordination numbers of O2,3 are smaller.

The bulk Ni hydroxide consists of a stack of 2-D $Ni(OH)_2$ sheet (see Fig.2). In the 2-D sheet, there are ferromagnetic interactions between Ni atoms. On the other hand, they exhibit an antiferromagnetic coupling between two adjacent sheets, leading to bulk antiferromagnetic property. From the difference in local structure and magnetization between bulk and cluster, we interpret the clusters as a 2-D monolayer-like structure. Since single 2-D monolayer possesses a ferromagnetic character, synthesized sample on the whole shows super-paramagnetism. The single 2-D monolayer has a smaller coordination number, which might be closely related to the reduction of the Ni-O1, Ni-Ni1 distances.

Table 1 Interatomic distances (Å) which are obtained from the EXAFS analysis. Number in ( ) shows errors of the last digit.

Sample	$Ni(OH)_2$ standard	$Ni(OH)_2$ cluster
Ni-O1	2.074(9)	2.060(7)
Ni-Ni1	3.129(3)	3.088(4)

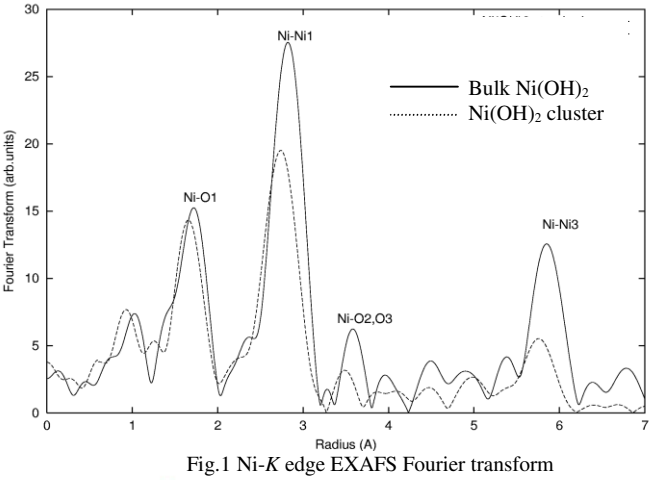

Fig.1 Ni-*K* edge EXAFS Fourier transform

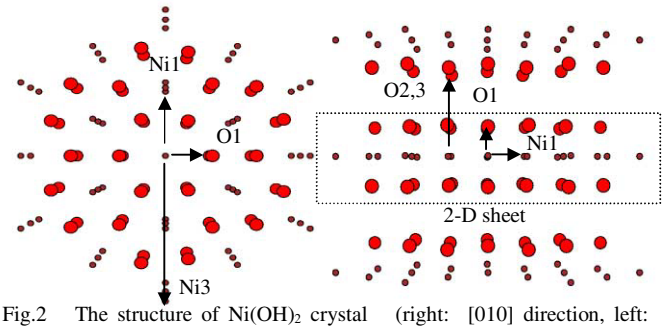

Fig.2 The structure of $Ni(OH)_2$ crystal (right: [010] direction, left: [001] direction) large circles: O, small circles: Ni, H is omitted. Dotted line: 2-D sheet

*ohta@chem.s.u-tokyo.ac.jp

10B/2001G092

Structural study of the effects of water and oxygen on the nitric oxide decomposition on $[Ru_6C]/TiO_2$ catalysts

Taketoshi Minato,[1] Yasuo Izumi,*[1] Ken-ichi Aika,[1] Atsushi Ishiguro,[2] Takayuki Nakajima,[2] Yasuo Wakatsuki[2]

[1] *Interdisciplinary Graduate School of Science and Engineering, Tokyo Institute of Technology, 4259 Nagatsuta, Midori-ku, Yokohama 226-8502*

[2] *Institute of Physical and Chemical Research, 2-1, Hirosawa, Wako, Saitama 351-0198*

Introduction

Various catalysts have been investigated to effectively decompose nitric oxide with reducing agent, such as ammonia, carbon monoxide, or hydrocarbons. In the practical applications of these catalysts, catalytic performance in the presence of moisture (water) and molecular oxygen is of primary importance. The presence of moisture and molecular oxygen has the possibility both to modulate the reaction mechanism and to modify the structure of catalyst active site. Due to this reason, in most cases it is not clear how these gases effect on the nitric oxide decomposition reactions. In this report, active site was defined by supporting ruthenium organometallic cluster $[(PPh_3)_2N]_2[Ru_6C(CO)_{16}]$ (**1**) on TiO_2. The active site structure was investigated by XAFS at Ru K-edge in the presence/absence of moisture/O_2. The effects of moisture and O_2 on catalytic nitric oxide decomposition with carbon monoxide are discussed.

Experimental Section

The cluster complex **1** was reacted at 290 K in tetrahydrofuran with TiO_2 (Aerosil P-25, BET surface area 60 m^2g^{-1}) previously heated in vacuum at 573 K. The solvent was evaporated. The Ru content was 1.5 wt%. The catalytic reaction was performed at 423 K in NO + CO (1 : 1, 4.0 kPa). 1.7 – 3.1 kPa of water and/or 0.56 kPa of O_2 were added to the reaction gas mixture. Ru K-edge XAFS was measured at 10B in transmission mode. All the procedure of catalyst preparation and transfer was carried out in argon atmosphere.

Results and Discussion

The decomposition reaction of nitric oxide proceeded by 6.0 – 23 times faster on $[Ru_6C]/TiO_2$ than the case of conventional Ru/TiO_2. As we reported in *Activity Report* 2000B, p.22, the active site structure was very similar to that of $[Ru_6C(CO)_{12}(NO)_3]^-$ crystal. The Ru_6 octahedral framework structure, stabilized by carbido carbon, was destroyed when the catalyst was heated above 523 K. The catalytic decomposition rate of nitric oxide once increased to 212% in the presence of 1.7 kPa of H_2O and then decreased to 31% in the presence of 3.1 kPa of H_2O in addition to the reaction gas of NO + CO. The change of Ru K-edge EXAFS (Fourier transform) is shown in Figure 1b by the addition of 3.1 kPa of H_2O. The Fourier transform is essentially the same as the case in the absence of water (a). Therefore, water did not modify the active site structure. When the adequate amount of water is adsorbed (1.7 kPa) on catalyst surface, it should be incorporated in the reaction mechanism, possibly the promotion of the decomposition step of isocyanate intermediate. However, excess amount of water adsorbed (3.1 kPa) may predominantly cover the Ru active site and retard the catalysis.

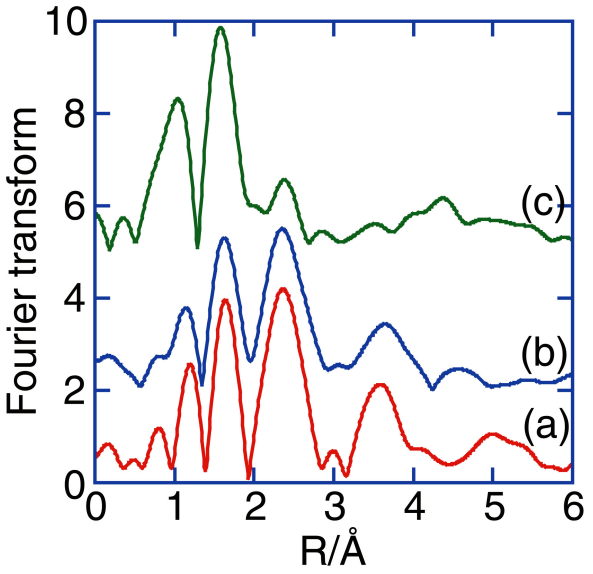

Figure 1. The Fourier transform of Ru K-edge EXAFS for $[Ru_6C]/TiO_2$ after the decomposition reaction of NO (2.0 kPa) with CO (2.0 kPa) was performed (a). 3.1 kPa of H_2O (b) or 0.56 kPa of O_2 (c) was added in addition to NO + CO.

The catalytic decomposition rate decreased to 51% in the presence of 0.56 kPa of O_2 in addition to NO + CO. The change of Ru K-edge EXAFS by the addition of O_2 is shown in Figure 1c. Compared to the case in the absence of O_2 (a), Ru-C-Ru peak at 3.7 Å (phase shift uncorrected) disappeared. The peak appeared at 1.6 Å was fitted well as the Ru-O bond at 2.02 Å (N = 1.6). Thus, the decomposition of $[Ru_6C]$ structure by O_2 is the reason of deactivation of the catalyst.

*izumi@chemenv.titech.ac.jp

10B/2001G094

XAFS study on structure of Ag species in MFI for HC-SCR in the presence of H_2

Junji SHIBATA*, Yuu TAKADA, Hisao YOSHIDA, Atsushi SATSUMA, Tadashi HATTORI
Department of Applied Chemistry, Graduate School of Engineering,
Nagoya University, Nagoya 464-8603, Japan

Introduction

Selective catalytic reduction of NO by hydrocarbon (HC-SCR) has received much attention because of its potential application to removal of NO_x from exhaust containing excess oxygen. Ag-containing zeolites show less activity for HC-SCR below 723 K [1]. Resently, we have reported that the low temperature activity of Ag/Al_2O_3 catalyst for the SCR by C_3H_8 is significantly improved by the addition of H_2 [2]. In the present study, we carried out the SCR by C_3H_8 in the presence of H_2 over Ag-MFI and investigated the structure of Ag species in MFI-type zeolite during the SCR by using XAFS.

Experimentals

Ag-MFI was prepared by a conventional ion-exchange of H-MFI (Tosoh, Si/Al = 22) with an aqueous $AgNO_3$ solution [1], followed by calcination at 773 K for 6 h in flowing dried air. The catalytic activity was measured with a fixed-bed flow reactor by passing a mixture of 1000 ppm NO, 1000 ppm C_3H_8, 10% O_2 and 0 or 0.5% H_2 in He at a rate of 100 cm^3 min^{-1} over 0.20 g of catalyst.

Ag K-edge XAFS spectra of Ag-MFI were measured at the BL-10B station [3] at KEK-PF with a Si(311) channel cut monochrometer in transmission mode at room temperature. Before measurements, the samples were treated with exposing various gas mixtures at 573 K for 30 min and were sealed in cells made of borosilicate.

Results and Discussion

The SCR by C_3H_8 in the absence and presence of H_2 over Ag-MFI was investigated. By the addition of H_2, NO conversion increased from 12 % to 50 % at 573 K. In the $NO+H_2+O_2$ reaction, however, reduction of NO by H_2 was not observed. This result indicates that H_2 is not a reducing agent but a promoter for the HC-SCR as well as Ag/Al_2O_3 [2].

Fig. 1 shows the Ag K-edge XANES spectra of Ag-MFI after the various treatments. XANES spectra of Ag-MFI after the treatment of NO + C_3H_8 + O_2 and of NO + C_3H_8 + O_2 + H_2 were different from those of Ag-MFI after O_2 treatment, Ag foil, Ag_2O and Ag_2SO_4.

Table 1 shows curve-fitting analysis on Fourier-filtered EXAFS of Ag-MFI. After O_2 treatment, only Ag-O shell at 2.06 Å was observed, which indicated that Ag was anchored within the micropores of the MFI zeolite in an isolated state [4]. After exposing the SCR atmosphere, particularly in the presence of H_2, Ag-Ag shell was observed. Coordination number and distance of Ag shell after exposing $NO+C_3H_8+O_2+H_2$ were 1.9 and 2.73 Å, respectively. This coordination number, lower than that of Ag foil, indicates formation of Ag cluster. From the previous literature [5], it is strongly suggested that Ag cluster are composed of Ag atoms from two to five.

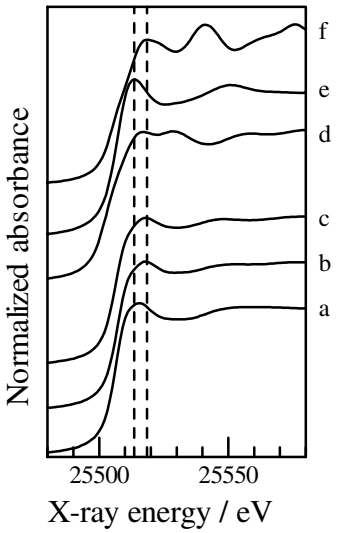

Fig. 1 Ag K-edge XANES spectra of Ag-MFI after treatment of (a) O_2, (b) $NO+C_3H_8+O_2$ and (c) $NO+C_3H_8+O_2+H_2$ at 573 K for 1 h, and those of (d) Ag_2O, (e) Ag_2SO_4 and (f) Ag foil.

Table 1 Curve-fitting results on Fourier-filtered EXAFS

sample	treatment	scatter atom	CN	r / Å	$\Delta\sigma^2$ / 10^{-3} Å^2
Ag-MFI	O_2	O	0.9	2.06	0.74
	$NO+C_3H_8+O_2$	O	0.5	2.07	2.25
		Ag	0.9	2.74	4.86
	$NO+C_3H_8+O_2+H_2$	Ag	1.9	2.73	3.34
Ag foil[1)]	—	Ag	12	2.89	—
Ag_2O[1)]	—	O	2	2.04	—

1) data from crystallography

References

[1] Z. Li et al., J. Catal., 182, 313 (1999).
[2] S. Satokawa, Chem. Lett., 294 (2000).
[3] M. Nomura et al., KEK Report 89-16, (1989).
[4] M. Anpo et al., Catal. Today, 39, 159 (1997).
[5] P. A. Montano et al., Chem. Phys. Lett., 164, 126, (1991)

* h011105d@mbox.media.nagoya-u.ac.jp

10B, 11B/2001G098

Location of Mo cations in HY zeolite prepared by decarbonylaton of $Mo(CO)_6$

Fusao Nakagawa, Takafumi Shido, and Yasuhiro Iwasawa*
Graduate School of Science, the University of Tokyo
Hongo, Bunnkyo-ku, Tokyo 113-0033, Japan

Introduction

To know the cation site in zeolite cages is indispensable to understand catalysis of cations in zeolites. The cation site has mainly studied by XRD and several cation exchange sites have been elucidated [1-3]. The drawback of XRD, however, is that it requires a long-range order, which are not possessed in many systems. On the other hand, EXAFS does not require such a long-range order and the cation site can be elucidated by a careful analysis of higher shell contributions. Recently, a theory including multiple scattering has been developed (FEFF8 [4]) and higher shell contributions can be reproduced by theoretical calculation.

The goal of this study is to determine the Mo cation site in HY zeolite prepared by decarbonylation of $Mo(CO)_6$ by higher shell analysis of EXAFS data. We have simulated Mo-K edge EXAFS functions for Mo cations located at several sites and compared them with observed data.

Experimental

Mo/HY sample was prepared as follows: $Mo(CO)_6$ was introduced into HY zeolite which was evacuated at 723 K by CVD at room temperature. Then the sample was evacuated at 573 K to remove CO ligands. The cycle of CVD-thermal decarbonylation was repeated for several times.

Mo K edge EXAFS spectra were measured at BL-10B at room temperature. After background subtraction, k^3 weighted EXAFS functions were Fourier transformed into a R space (k range = 3.0-12.0 A^{-1}) and the first shell was analyzed by curve fitting. In addition, higher shell contributions were analyzed by the simulation of the EXAFS function using the FEFF8 code.

Result and discussions

Figure 1 (a)–(c) show Fourier transformed EXAFS functions of decarbonylated Mo/HY (1-3 cycles). Phase shifts are not corrected in this figure. For decarbonylated sample, Mo-O contribution was observed at 0.16 nm, and higher shell contributions were observed at 0.22, 0.24, and 0.38 nm. The EXAFS functions of decarbonylated Mo/HY sample was very similar up to three cycles, which suggests that the local structure of the Mo species in HY cages are homogeneous. This allows us to determine the cation site by a careful analysis of higher shells. To determine the cation site, we have simulated Mo K edge EXAFS functions of Mo cations at a certain position in the cages. To simulate EXAFS functions, a Mo cation was located in the cages of HY zeolite and moved the adjacent oxygen atoms so that Mo—O distance satisfied the result of conventional curve fitting for the first shell. A Debye model was used to estimate the Debye Waller factors for the higher shells. Figure 2 shows the position of Mo cation determined by the simulation. The simulation revealed that the Mo is near S3' site. Other site cannot reproduce the observed EXAFS function. This is the first study that determines the cation site by EXAFS.

References

[1] E. Jaramillo and S. Auerback, *J. Phys. Chem. B* **103** 9589 (1999).
[2] G. Vitale, C. Mellot, L. Bull, and A. Cheetham, *J. Phys. Chem. B* **101** 4559 (1997).
[3] G. Marra, A. Fitch, A. Zecchina et al., *J. Phys. Chem. B* **101** 10653 (1997).
[4] A. L. Ankudinov, B. Ravel, J. J. Rehr, and S. D. Conradson, *Phys. Rev. B* **58**, 7565 (1998).

*iwasawa@chem.s.u-tokyo.ac.jp

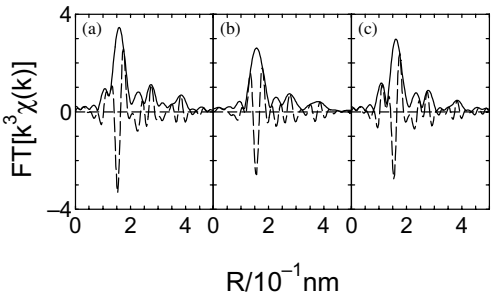

Figure 1. Fourier transformed EXAFS functions for decarbonylated Mo/HY. (a) 1 cycle, (b) 2 cycles, and (c) 3 cycles.

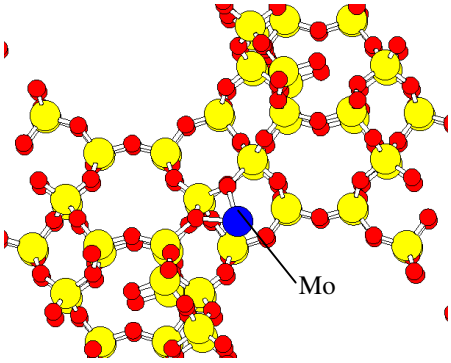

Figure 2. Positin of Mo cation determined by EXAFS analysis.

7C, 9A, 12C/2001G102

Chemical speciation of heavy metals in the estuarine and tideland sediments

Masaki KATAOKA*[1] and Motoyuki MATSUO[2]

[1]Graduate School of Science, The University of Tokyo,
3-8-1 Komaba, Meguro-ku, Tokyo 153-8902, Japan
[2]Graduate School of Arts and Sciences, The University of Tokyo,
3-8-1 Komaba, Meguro-ku, Tokyo 153-8902, Japan

Introduction

A brackish-water area including an estuary and a tideland is a very complicated system in which fresh water and seawater are mixed. Accordingly, the distribution, mass transfer and chemical change of elements in their sediments have not been well understood. Yatsu tideland is located at Narashino-city, Chiba Prefecture, Japan. Yatsu tideland was assigned to a conservation area, so people could not enter without admission. Because of it, the sediment of Yatsu tideland is preserved as it was and non-polluted, compared with other estuaries and tidelands. Several studies of estuarine area in the vicinity of big cities were carried out, including Tokyo bay area. But the non-polluted brackish-water area that is located at the vicinity of big cities is rare. Therefore, information on their sediments is significant for comparison with nearby estuarine and tideland areas. In estuarine and tideland sediments under anaerobic condition, sulfate ion from seawater is reduced to hydrogen sulfide. Environmental problem was occurred, because hydrogen sulfide is one of malodorous substances. Hydrogen sulfide reacts with heavy metals(iron and manganese mainly) and is removed from water to the sediments in the forms of sulfide. We have already investigated the chemical states of iron by Moessbauer spectroscopy [1].

In this study, XAFS spectroscopy has been applied to the sediments in order to directly investigate the change in chemical states of manganese with depth.

Experimental

Sediment samples were collected from the Yatsu tideland which is located in Tokyo bay area. The collected sediments were cut at every 3 cm length immediately, and then porewater was removed by pressure filtration (5 atm, N_2). Approximately 300mg of each sample was mounted in a sample holder. In order to avoid air oxidation, the sediments were purged with nitrogen gas in oxygen-impenetrable plastic bags. The X-ray absorption measurement was made with synchrotron radiation by using XANES facilities on the beam line 7C, 9A and 12C. The radiation was monochromatized by Si(111) double crystals. The spectra were collected in fluorescence mode using Lytle-type detector at room temperature.

Results and Discussion

Figure 1 shows the normalized Mn K-XANES spectra of the Yatsu tideland sediments from different depths and standard materials of manganese. According to the comparison with the standard materials, manganese in the sediments existed as mixture of divalent and trivalent components. From the shape of each spectrum at 6.545 keV, MnS was estimated to be rich only in the surface layer, because only the spectrum of the sediment of surface layer has a peak at highest normalised absorption coefficient point of MnS spectra. In our previous research, the vertical distribution of manganese did not show significant variation, but manganese increased a little in the surface layer [1]. According to this fact, it may be imagined that the accumulation of MnO_2(oxidation number of manganese is four) was generated under an oxidative condition. However, our results clearly show the oxidation state of manganese is not tetravalent. Therefore, it is suggested that manganese in the surface layer reacts with hydrogen sulfide and is accumulated in the form of MnS.

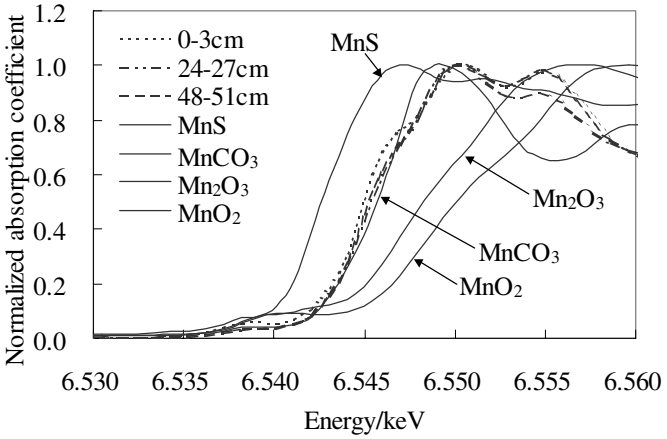

Fig. 1. Normalized Mn K-XANES spectra of the Yatsu tideland sediments and standard materials

References

[1] M.Kataoka et al., J. Radional. Nucl. Chem., in press (2002).

* kataokai@dolphin.c.u-tokyo.ac.jp

11A, 27A/2001G107

Local structures in graphite-like carbon oxide

Iwao SHIMOYAMA, Tetsuhiro SEKIGUCHI, Yuji BABA
Japan Atomic Energy Research Institute, Tokai-mura, Naka-gun, Ibaraki-ken, 319-1195, Japan

Introduction

Carbon oxide is one of the basic materials in chemistry. Besides CO and CO_2, some kinds of carbon oxide are also known. All of them are gas or liquid at ambient temperature and pressure, and it is believed that stable solid carbon oxide does not exist. In this work, for the quest of solid carbon oxide (CO_x), we attempted to synthesize CO_x by ion implantation. Though this method is superior in synthesis of novel materials via non-equilibrium process, variety of possible local structures could be formed and long-range order is expected to be lacking due to the damage induced by the incident particles. Then we studied local structures of the products around oxygen sites by XPS and NEXAFS spectroscopy.

Experimental

XPS and NEXAFS experiments were performed at BL-27A and BL-11A, respectively. All experiments were carried out *in situ* to avoid the contaminant effect. CO_x films were prepared by low energy (1-3keV) O_2^+ ion implantation in highly oriented pyrolitic graphite at room temperature. XPS spectra were measured by monochromatic 1.8 keV x-ray with the resolution of 0.9 eV. The composition ratio of the products was obtained from XPS. As references, the O 1s binding energies (BE) of 18-crown 6-ether powder and condensed γ-pyrone, furan, CO_2, and tetramethoxymethane (TMM) were also measured. NEXAFS spectra were measured by total electron yield mode for various x-ray incident angles. To minimize the damage effect, NEXAFS spectra of the CO_x film were measured at low fluence (1.7×10^{15} atoms/cm^2). O *K*-edge NEXAFS spectra of condensed furan and diethylether were measured. A few monolayer of γ-pyrone was adsorbed on Cu(100) at 250 K and NEXAFS spectrum of this system was also measured.

Results and discussion

The [O]/[C] ratio of the CO_x film reached up to 13% at the fluence of 1×10^{17} atoms/cm^2. As compared with the [Ar]/[C] ratio (≈ 4%) in the case of Ar^+ ion irradiation, the value is quite large. As shown in figure 1, two dominant and one minor components P_1, P_2, and P_3 are observed in the O1s XPS spectrum. CO_2 ice (dry ice) is well known as molecular solid of carbon oxide, and the O 1s BE is by far different from the energies of P_1 and P_2 and close to that of P_3. The O 1s BEs of the most reference materials in which ether are included are rather closer to the energy of P_2 than that of P_1. γ-pyrone showed two O 1s BEs corresponding to different oxygen sites, *i.e.*, carbonyl group and ether, which are close to those of P_1 and P_2 respectively. These results imply that the dominant products are not interstitial carbon oxide compound but carbonyl or ether structures in graphite matrix. As shown in figure 2 (curves a-c), the O *K*-edge NEXAFS spectra of the CO_x show two discrete peaks P_a and P_b which have graphite-like clear polarization dependence. This implies that the local structures corresponding to the peaks have orientation which is parallel to graphite plane. The energies of the peaks coincide with the two π* resonances in O *K*-edge NEXAFS spectrum of condensed γ-pyrone (curve d). Among the peaks, the high-energy peak correspond to the π* resonance of furan (curve e). On the other hand, diethylether did not show discrete π* resonance in the spectrum (curve f). This means that P_a and P_b are assigned to the π* resonances which originates from carbonyl groups and ether structures in graphite plane. Consequently, we propose a structural model of the CO_x film as shown in figure 3. When ion fluence is small, graphite crystal structure would be preserved. In this situation, the orientation of carbonyl groups is parallel to graphite basal plane and form quinone-like structure. Ether lies in graphite basal plane and has graphite-like orientation.

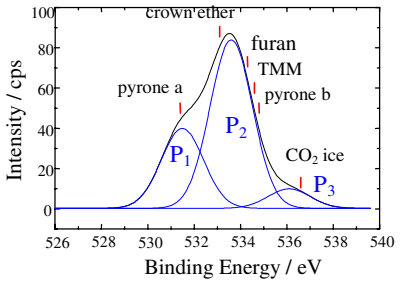

Figure 1 (up). O1s XPS spectrum of the CO_x film synthesized at the ion fluence of 3.4×10^{17} atoms/cm^2. Bars show the binding energies of reference materials.

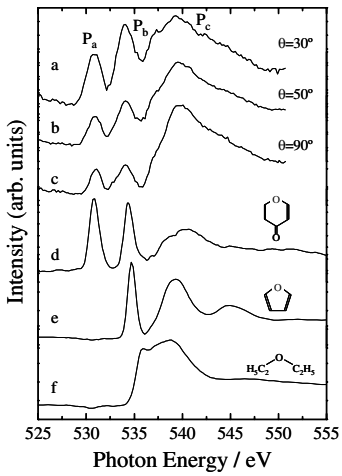

Figure 2 (center). O *K*-edge NEXAFS spectra of the CO_x film and reference materials. θ shows x-ray incident angle.

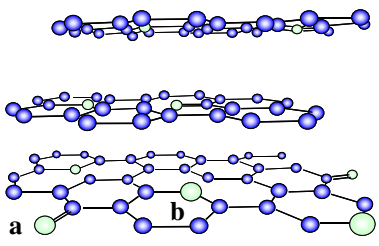

Figure 3. Schematic figure of local structures in the CO_x film synthesized at low fluence. White and dark balls show oxygen and carbon atoms, respectively. **a**: quinone-like structure, **b**: in-plane ether structure

9A/2001G117

X-ray induced polymerization of Si resin and reduction of Pt catalysts

Kiyotaka Asakura*[1] and Mamoru Tachikawa[2]
[1]CRC, Hokkaido University Sapporo 060-0811, Japan
[2]Dow Corning Asia , Yamakita 603, Kanagawa, 258-0112, Japan.

Introduction

Pt catalysts are important for hydrosililation reactions. We have studied the structure of Pt catalysts during the reaction and extended our work to the retardation effects of bismaleate which are important for the control of the solidification of the silicon resin. During the work we found that the X-ray radiation-induced the polymerisation reaction accompanied by the reduction of Pt catalysts. In order to carry out the structural analysis of the Pt catalysts, we first revealed the origin of the observed X-ray irradiation effect on the structure of Pt catalysts.

Experimetnal

The EXAFS measurements were carried out at BL9A.

The sample including Pt catalyst, bismaleate, vinylpolydimethylsiloxane and polydimethylsiloxane. Bismaleate is a retardor of the reaction. In order to see the structural change of the Pt catalysts during the reaction we varied the reaction times and temperatures and we followed the structure change of Pt in the reaction processes.

Results and Discussion

Fig. 1 shows the XANES of Pt L_3 edge soon after the X-ray irradiation (A) and 2 hours after the continuous measurement(B). The spectra changes with the exposure time to X-ray. The analysis of EXAFS indicated the agglomeration of Pt to form Pt clusters. At the same time, the resin was hardened at the irradiated spots. Thus the X-ray irradiation induced the polymerization reaction. There are two possibilities for the radiation effect. One is the excitation of Pt L_3 edge which initiates the catalytic reaction of polymerization. The other is the radical reaction formed from the solvent or reactants by the irradiation of X-ray. To confirm this point, we carried out the EXAFS measurement at 11400 eV a little lower energy than the Pt L_3 edge for 2 hours. Fig.1C shows the XANES spectra, indicating the reduction of Pt occurred together with the polymerization reaction. Thus the latter possibility is more plausible.

In order to reduce the polymerization reaction, we carried out the experiment at lower temperature than 70 K. However, we could not inhibit the reaction. Thus the activation energy for the polymerization reaction induced by X-ray is very low. This can be rationalized by the hot atom formation by the high energy X-ray. Thus we carried out the XAFS measurements with a short time and accumulated the data by changing the position with every scan. Finally we obtained the data at the initial stage. The Pt-C bond was found at 0.220 nm as shown in Fig.2. Further analysis is now going on and we will try to determine the interaction between retardor and Pt catalyst.

This work has revealed that focused and intense X-ray may change the sample and we have to be more careful about the radiation damage.

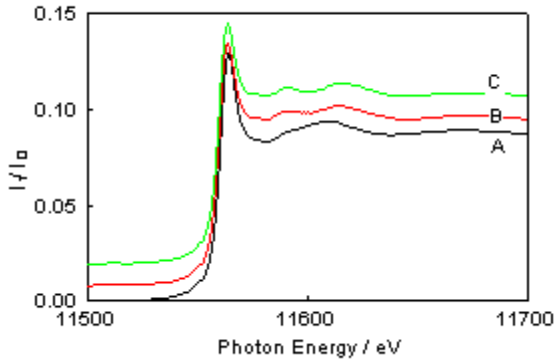

Fig.1 Radiation damage of Pt complex just after the irradiation (A), 2 hours after the continuous measurements(B), and 2 hours after the X-ray irradiation with 11 KeV less than Pt L3 edge(C).

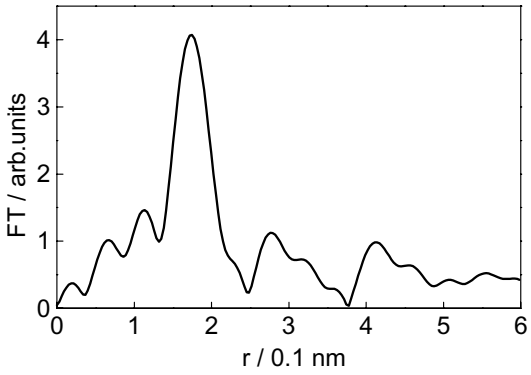

Fig. 2 Fourier transformation of the Pt catalyst soon after the reaction.

* askr@cat.hokudai.ac.jp

12C/2001G122

Structural change of REE coprecipitated with Fe-Mn oxyhydroxides

Atsuyuki OHTA[1], Hiroshi TSUNO[2], Hiroyuki KAGI*[3], Yoshio, TAKAHASHI[4], Masaharu, NOMURA[5], Iwao KAWABE[6]

[1]Geological Survey of Japan, AIST, Tsukuba, Ibaraki 305-8567, Japan
[2] Institute for Environmental Management Technology, AIST, Tsukuba, 305-8569, Japan
[3]The University of Tokyo, Tokyo 113-0033, Japan
[4]Hiroshima University, Hiroshima 739-8526, Japan
[5]Institute of Materials Structure Science, KEK, Ibaraki 305-0801, Japan
[6]Naogya University, Aichi 464-8567, Japan

Introduction

Ohta et al. [1,2] and Ohta and Kawabe [3] have experimentally and theoretically studied the partitioning reaction of rare earth element (REE) between Fe-Mn deposit and seawater. When analyzing their distribution coefficients theoretically, we need to correct the structural changes, because lanthanide (Ln) complexes are not usually isomorphous in the entire Ln series. Ohta and Kawabe [3] pointed out 1) the proportion of hydroxyl ions to the others ligating REE ions scavenged by δ-MnO_2 increases with solution pH, 2) the preferential adsorption of light Ln onto δ-MnO_2 is obvious compared with their adsorption onto FeOOH. We focus the latter case and have tried to characterize the local structure of Ln adsorbed with δ-MnO_2 and FeOOH with XAFS spectroscopy.

Method

The experimental method was based on the report of [1,3]. Iron(III) oxyhydroxide (FeOOH) and manganese dioxide (δ-MnO_2) were formed and react with La(III) or Nd(III) in 0.5 M NaCl solutions with 1.3 mM $NaHCO_3$. These precipitates were gently stirred with magnetic stirrers in glass flasks placed in a water bath with 25 °C. After 4 or 5 days, the precipitates were filtrated with polycarbonate membrane filters. The precipitates were dried at 40-50 °C and preserved in plastic bags.

The La-L_{III} and Nd-L_{III} XAFS spectra were recorded in the fluoresce mode at the BL12C of KEK-PF [4] under the atmosphere and at room temperature. The fluoresce X-ray was measured by a 19 element pure-Ge SSD [5]. Analysis of the XAFS spectra was performed with a PC program, REX2000 (Rigaku co.).

Result and Discussion

The δ-MnO_2 and FeOOH adsorbing La or Nd are expressed as Ln/ δ-MnO_2 and Ln/FeOOH (Ln = La and Nd). The Ln/ δ-MnO_2 has a quite similar XANES spectra to Ln/FeOOH. This result indicates that the chemical compound of Ln adsorbed onto δ-MnO_2 is almost as same as those with FeOOH: $Ln(OH)_3$ nH_2O.

The EXAFS spectra of Ln/δ-MnO_2 also are not particularly different from those for Ln/FeOOH. Fig. 1 shows the Fourier transform of $k^3\chi(k)$ of Ln/ δ-MnO_2 and Ln/FeOOH. The curve-fitting results were summarized in Table 1. Fourier transformed spectra of Ln/ δ-MnO_2 and Ln/FeOOH have one large peak at 2Å (no phase-shift correction). The fitting results of first shell (La-O and Nd-O) suggested that the coordination number of Ln coprecipitated with δ-MnO_2 is possibly different from those with FeOOH (Table 1). This result indicates that the preferential adsorption of light Ln onto δ-MnO_2 is caused by the increase of their hydration numbers.

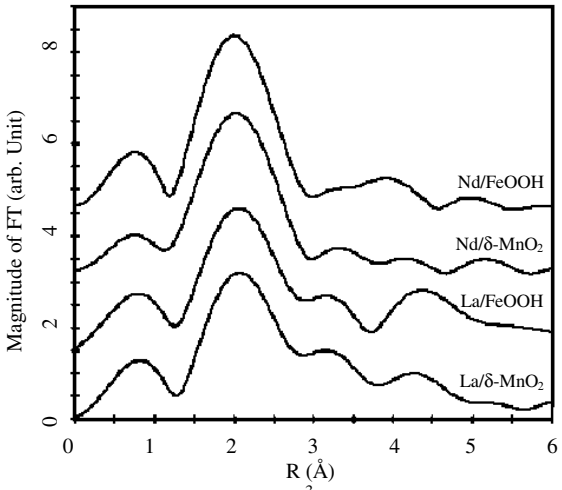

Fig. 1 Fourier transform of k^3 weighted La and Nd L_{III} EXAFS of FeOOH and δ-MnO_2 adsorbing La and Nd. The phase shift is uncorrected.

Table 1: Curve-fitting results for Ln incorporated with FeOOH or δ-MnO_2.

Samples	CN	R_{Ln-O}/Å	DW/ Å
La /FeOOH	7.35	2.57	0.117
Nd / FeOOH	7.37	2.51	0.101
La / δ-MnO_2	7.82	2.58	0.120
Nd / δ-MnO_2	7.87	2.51	0.108

References

[1] Ohta A. et al. (2000a), Geochem. J. 34, 439-454.
[2] Ohta A. et al. (2000b), Geochem. J. 34, 455-473.
[3] Ohta A. and Kawabe I. (2001), Geochim. Cosmochimi. Acta 65, 695-703.
[4] Nomura, M. and Koyama, A., KEK Report, 95-15, 1 (1996)
[5] Nomura, M., KEK Report, 98-4, 1 (1998).
* kagi@eqchem.s.u-tokyo.ac.jp

12C/2001G131

Characterization of iron in airborne particulate matter by XANES technique

Motohiro HIRABAYASHI*[1], Motoyuki MATSUO[2], Kiyoshi TANABE[3], Masaharu NOMURA[4]
[1]Department of Chemistry, Graduate School of Science, The University of Tokyo, Meguro-ku, Tokyo 153-8902, Japan
[2]Department of Chemistry, Graduate School of Arts and Sciences,
The University of Tokyo, Meguro-ku, Tokyo 153-8902, Japan
[3] Environmental Chemistry Division, National Institute for Environmental Studies, Tsukuba, Ibaraki 305-8506, Japan
[4]Photon Factory, Institute of Materials Structure Science, KEK, Tsukuba, Ibaraki 305-0801, Japan

Introduction

Elucidating the chemical property and dynamic change process of airborne particulate matter is important. Metal complex in airborne particulate matter needs to be investigated in order to asses the chemical reaction on its surface. Iron is one of the most abundant elements in airborne particulate matter. Iron compounds are introduced from various natural and, at the same time, anthropogenic sources into the atmosphere. The chemical species of iron in airborne particulate matter are reported very widely according to origin, such as soil and exhaust of combustion engines, by ^{57}Fe Mössbauer spectroscopy. Therefore, for identifying the origins of aerosol, the chemical states of iron in airborne particles merits investigation. In this report, we have applied XANES to characterize the chemical states of iron in particulate matter samples. In addition, an attempt was made to quantify the chemical species of iron in airborne particles by applying partial least-squares (PLS) method [1].

Experimental

The sampling was carried out at the campus of The University of Tokyo in early October 2000. This sampling site is located in urban area in Tokyo, Japan. Airborne particles were collected by four-staged Andersen air sampler equipped with a back-up filter. The standard reagents, the mimetic chemical compounds for supposed form of iron compounds in airborne particles, were measured to compare with the airborne particle samples. The standard chemical reagents, whose chemical species are olivine ($(Fe,Mg)_2SiO_4$), iron (III) sulfate ($Fe_2(SO_4)_3$) and iron (III) oxide (Fe_2O_3) were also used for PLS modeling.

The XAFS measurement was performed using synchrotron radiation ring at BL-12C, Photon Factory, KEK, Japan [2]. A Si (111) double-crystal monoclometer was used. The iron K-edge XANES spectra of the samples were measured in a fluorescence mode using a Lytle-type detector.

Results and Discussion

The XANES spectra of olivine, iron (III) sulfate and iron (III) oxide which were selected as model compounds seem to cover almost the whole range, where the spectra of airborne particles lie. The absorption edge of fine particle shifted towards higher energy than that of coarse particle. The oxidation state of iron species increases with decreasing grain sizes, and increasing with contribution of anthropogenic effects. From this fact, it is suggested that the edge energy of spectrum is regarded as an index of anthropogenic effects. Figure 1 shows relative abundance of iron species estimated from the PLS calculation. Relative abundance of Fe (II) component decreases with a decrease in grain size. Most Fe (II) is found in nature as silicates and the size of the particles in which Fe (II) is found is usually larger compared with grain sizes where Fe (III) is dominated.

In this work, we were able to estimate the relative abundance of chemical species of iron by applying PLS modeling to XANES data. This paper can be possible path way to wider application of XANES and PLS modeling to chemical speciation of metals in airborne particle samples.

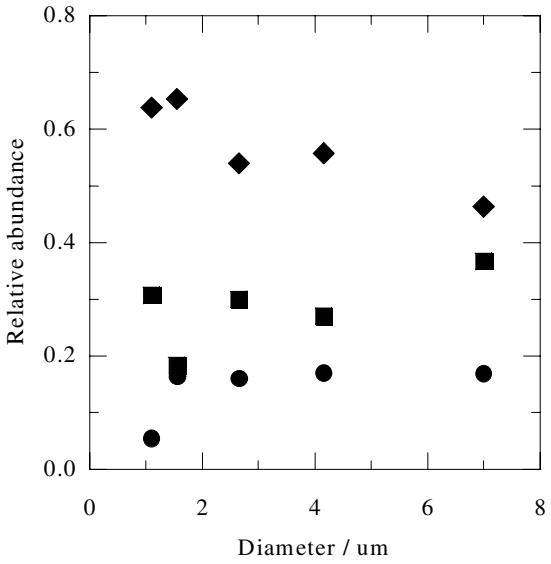

Figure 1. Relative abundance of iron species in airborne particles as determined by PLS modeling: ● , ferrous silicates (olivine); ■ , ferric sulfate ($Fe_2(SO_4)_3$); and ◆, iron oxide (Fe_2O_3).

References

[1] H. Hirabayashi et al., Anal. Sci., **17**, i1581 (2001).
[2] M. Nomura, KEK Report, 95-15 (1996).

* ss17167@mail.ecc.u-tokyo.ac.jp

10B/2001G138

Local structure analysis of zeolite-supported Ni and Co sulfide catalysts possessing a high HDS activity by means of X-ray absorption spectroscopy

Takeshi KUBOTA*[1], Yasuaki OKAMOTO[1]
[1]Department of Material Science, Shimane-Univ.,
Matsue, Nishikawatsu, Shimane 690-8504, Japan

Introduction

Recently, regulation of sulfur content in light oil has become severer to reduce particulate materials and SO_x in exhaust. For these purposes, development of new catalysts for ultra-deep-HDS treatment is strongly needed now. Currently, Co-Mo sulfide catalysts are used for HDS treatment. Recently, it was reported that Co sulfide catalysts supported on smectite, NaY and USY zeolite also show high HDS activities. Since these Co sulfide catalysts are supported on high-surface area supports, it is assumed that high dispersion of Co sulfides causes their high HDS activities. It is of great importance to study the catalytic properties of atomically dispersed Co sulfide species to disclose the origin of the catalytic synergies between Co and Mo sulfides and to provide rational bases for the design of highly active HDS catalysts. In this study, we report local structure of highly dispersed Co and Ni sulfide clusters supported in Na-type zeolites.

Experimental

Co/USY, Ni/NaY and Ni/USY catalysts were prepared by an impregnation method using $Co(NO_3)_2$ and $Ni(NO_3)_2$. The sample was sulfided at 673 K. The sulfided sample was evacuated at 673 K and transferred to an EXAFS cell with two Kapton windows without exposing to air. Co and Ni K-edge EXAFS spectra were measured at BL-10B in a transmission mode. The synchrotron radiation was monochromatized by a Si(311) monochromator.

Results and Discussion

Fig.1 shows Co K-edge XANES spectra for Co sulfide catalysts. The spectrum of CoS/USY-Na catalyst prepared by the impregnation method shows a sharp peak about 7725 eV. The peak intensity is stronger than that for CoS_x/USY-Na catalyst prepared by the CVD method. This result indicates that Co sulfides in the catalyst prepared by the impregnation method interact with the acid sites of the zeolite according to the following equation.

$$CoS + 2H^+(s) \rightarrow Co^{2+} + H_2S \uparrow$$

Fig.2 shows Ni K-edge XANES spectra for Ni sulfide catalysts. The spectrum of NiS/NaY catalyst prepared by an ion-exchange method shows very strong peak about 8355 eV. But the intensity of the peak for NiS/USY-Na and NiS/NaY catalysts prepared by the impregnation method are very weak. This is due to the variation in the amount of acid sites of zeolite and the reaction of Ni sulfide clusters with them.

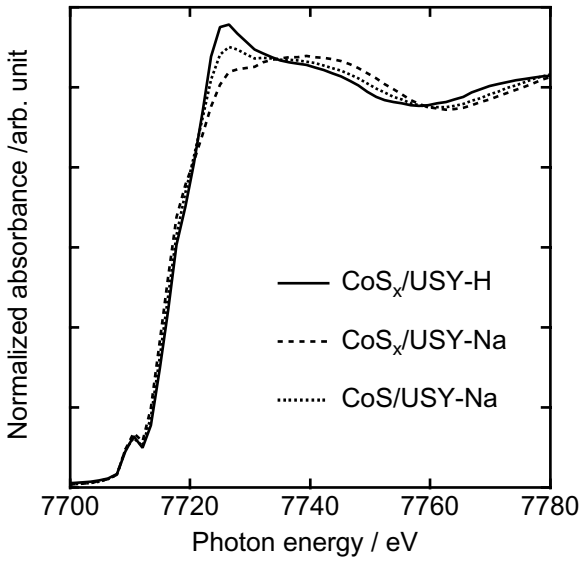

Fig.1 Co K-edge XANES spectra for Co sulfide catalysts prepared by an impregnation method and a CVD method.

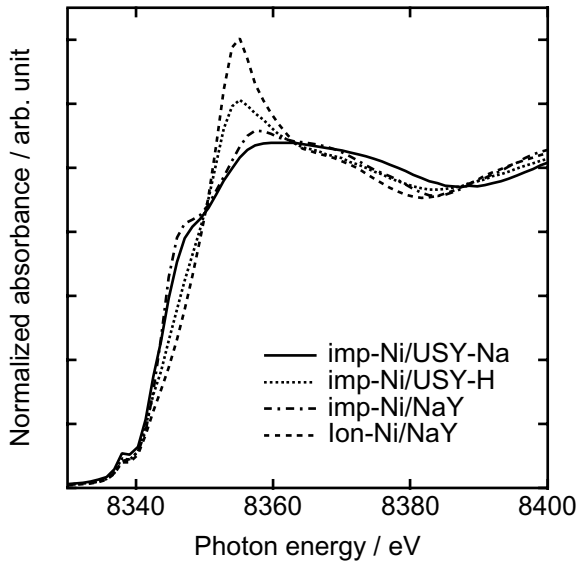

Fig.2 Ni K-edge XANES spectra for Ni sulfide catalysts prepared by an impregnation method and an ion-exchange method.

*kubotake@ifse1.riko.shimane-u.ac.jp

10B, 12C/2001G139

Local structure analysis of supported Co-Mo binary sulfide catalysts prepared by a CVD method by means of X-ray absorption spectroscopy

Takeshi KUBOTA*[1], Takao KAWABATA[1], Keiji OCHIAI[1], Yasuaki OKAMOTO[1]
[1]Department of Material Science, Shimane-Univ.,
Matsue, Nishikawatsu, Shimane 690-8504, Japan

Introduction

Currently, Co-Mo sulfide catalysts are used for HDS treatment. It is well known that catalytic synergy generates between Co and Mo sulfides in the catalyst system. As a result of numerous studies to clarify the cause of the synergy effects by means of a variety of physicochemical techniques, it has been proposed that a "Co-Mo-S" phase is responsible for HDS activity. But conventional catalyst preparation methods cause the formation of other Co species besides "Co-Mo-S" phase. Thus a new preparation method is desired to effective formation of Co-Mo-S phase. It is expected that a selective decoration of metal sulfide catalysts and synthesis of atomically controlled metal sulfide cluster are realized by a CVD method using metal carbonyl clusters. In this study, we investigated the structure of supported Co-Mo sulfides prepared by a CVD method by means of XAFS.

Experimental

CoS_x-MoS_2/support (support: SiO_2, Al_2O_3, TiO_2, ZrO_2) catalysts were prepared by a CVD method using $Co(CO)_3(NO)$. CoS_x-MoS_x/zeolite (zeolite: NaY, USY) catalysts were prepared by a CVD method using $Mo(CO)_6$ and $Co(CO)_3(NO)$. The sample was sulfided at 673 K. The sulfided sample was evacuated at 673 K and transferred to an EXAFS cell with two Kapton windows without exposing to air. Mo K-edge XAFS spectra were measured at BL-10B (Si(311)) in a transmission mode. Co K-edge XAFS spectra were measured at BL-12C (Si(111)) in a fluorescence mode.

Results and Discussion

Fig.1 shows Fourie transforms of the EXAFS oscillation of Co K-edge EXAFS for Co-Mo sulfide catalysts. Co atoms in the CVD method form highly dispersed sulfide clusters. In the catalyst prepared by an impregnation mehtod, Co-O shell is observed, being different from CVD-prepared catalysts. This result indicates selective formation of Co-Mo-S phase by the CVD method. Fig.2 shows Fourie transform of EXAFS oscillation of Mo K-edge EXAFS of Mo and Co-Mo sulfide catalysts prepared by a CVD method. The strucure of Mo sulfide clusters in NaY zeolite is affected by the Si/Al ratio. Namely, by using high Si/Al ratio (2.8) NaY as a support, Mo-Mo shell is shifted to a shorter bond distance. However, the cluster structure becomes identical by complexing Co and Mo. It is considered that cuban-type Co-Mo binary cluster is synthesized in zeolite super cages.

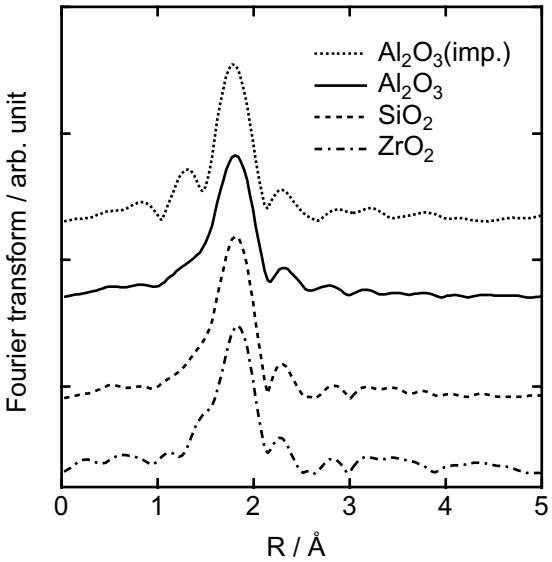

Fig.1 Fourie transform for EXAFS oscillation of Co K-edge EXAFS of Co-Mo sulfide catalysts prepared by a CVD method and an impregnation method.

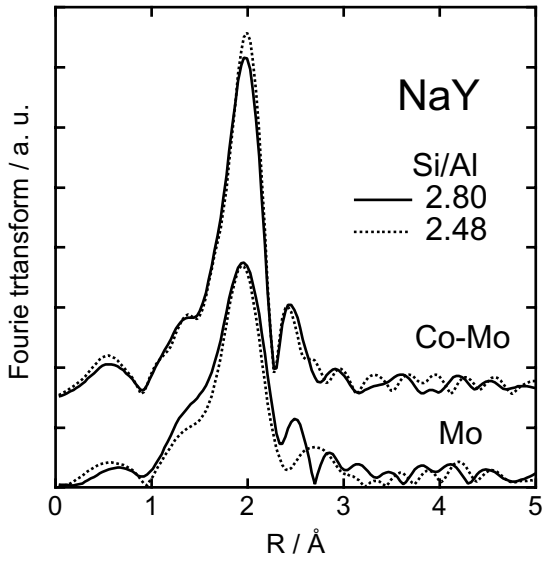

Fig.2 Fourie transform for EXAFS oscillation of Mo K-edge EXAFS of Mo and Co-Mo sulfide catalysts prepared by a CVD method. Catalysts supports (NaY zeolite) are different in Si/Al ratio.

*kubotake@riko.shimane-u.ac.jp

27B/2001G140

Structural study of zirconium in aqueous solution for transactinide element research

Kazuaki TSUKADA*[1], Hiromitsu HABA[1], Masato ASAI[1], Kazuhiko AKIYAMA[1], Tsuyoshi YAITA[1], Hirokazu NARITA[1], Atsushi TOYOSHIMA[2], Ichiro NISHINAKA[1], Yuichiro NAGAME[1]

[1]Japan Atomic Energy Research Institute, Tokai, Ibaraki 319-1195, Japan

[2]Osaka University, Suita, Osaka 565-0871, Japan

Introduction

According to the actinide concept, the 5f electron series ends with element 103, lawrencium (Lr), and a new 6d transition metal, transactinide, series is predicted to begin with element 104, rutherfordium (Rf). So far, we have studied an anion-exchange behavior of Rf homologues together with the lighter Zr and Hf in HCl. The results have clearly shown that the behavior of Rf is quite similar to that of Zr and Hf, indicating Rf is the member of the group 4 elements [1]. To discuss the anion structure of Rf, Zr and Hf in HCl, we study structure of Zr in various concentration of HCl with the EXAFS method.

Experimental

$ZrCl_4$ were dissolved with 1 M to 11.5 M HCl. The concentration of Zr was adjusted to 0.01 M for each sample solution. Each sample was sealed in a polyethylene bag and set to the beam line of BL27B. The Zr-K edge EXAFS spectra were measured with the fluorescence mode using a 7-element pure-Ge solid state detector.

Results and Discussion

The Fourier transformed EXAFS spectra of the Zr-K edge are shown in Fig. 1, in which the phase shifts were not corrected. In the range of 1 to 10 M HCl, the most intense peak is observed at 1.77 Å that corresponds to the distance of the Zr-O bond. At > 9 M HCl, this peak broadens with the concentration of HCl due to the increase of the condition from the Zr-Cl bond at 2.0 Å. In 1 M to 5 M solution, the peak observed at 1.25 Å is originated from Z=O and its intensity decreases with the concentration of HCl. While in 1 and 3 M solution, an extremely characteristic peak derived from Zr-Zr is observed at 3.3 Å. This suggests that Zr forms a binuclear complex in these low concentrations. Thinking about the decrease of the intensity of the Zr=O peak and the growing up of the Zr-Cl peak with the HCl concentration, it is suggested that a Zr anion, such as $[ZrCl_6]^{2-}$, is produced in the higher concentration of HCl solution by the substitution of the Zr=O to the Zr-Cl in terms of the insertion of Cl^- ions to the coordination positions. These dramatic changes of the ligands in the Zr anion provide the good account for the result of the adsorption behavior of Zr on the anion exchange resin [1]. In the next experiments, we will try to reveal the structure of Hf in HCl solution.

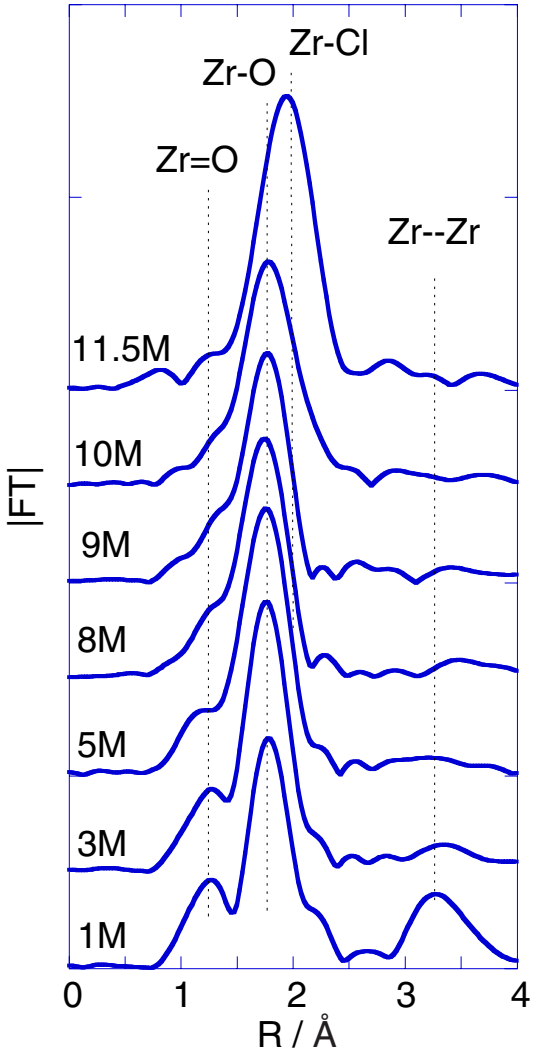

Figure 1. Fourier transformed EXAFS spectra of Zr-K edge:

Reference

[1] H. Haba et al., J. Nucl. Radiochem. Sci. **3**, 143 (2002).

* ktsuka@popsvr.tokai.jaeri.go.jp

9A,10B,12C/2001G141

Photo-induced magnetized state of Co(DTBSQ)(DTBCat)(phen)·$C_6H_5CH_3$ studied by X-ray absorption spectroscopy

Toshihiko YOKOYAMA*[1], Kaoru OKAMOTO[2], Kensuke NAGAI[2], Toshiaki OHTA[2], Shinya HAYAMI[3], Zhong-Ze GU[3], Rie NAKAJIMA[3] and Osamu SATO[3]
[1]Institute for Molecular Science, Okazaki, Aichi 444-8585, Japan
[2]Dept. Chemistry, Graduate School of Science, The Univ. of Tokyo, Hongo, Tokyo 113-0033, Japan
[3]KAST, KSP East 412, 3-2-1 Sakado, Takatsu-ku, Kawasaki-shi, Kanagawa 213-0012, Japan

Introduction

Recently Sato *et al*. found a photoinduced phase transition in Co(DTBSQ)(DTBCat)(phen)·$C_6H_5CH_3$ (DTBSQ=3,5-di-*tert*-butyl-semiquinone, DTBCat=3,5-di-*tert*-butyl-catechol and phen=1,10-phenanthroline) at low temperature. From the IR spectra it is suggested that the $DTBCat^{2-}$ anion is converted back to $DTBSQ^{-}$ after visible-light (532 nm) irradiation, indicating the charge transfer from $DTBCat^{2-}$ to Co(III). There seems to be two possibilities that account for the Co valency; one is Co(II)HS, the same as the HT phase, and the other is a new state of Co(II)LS.

In this work, we have measured and analyzed Co *K*-edge XANES and EXAFS to identify the photoinduced phase [1].

Experimental

The Co *K*-edge XAFS spectra of the low-temperature (LT) and high-temperature (HT) phases were recorded with the transmission mode at BL10B, while those of the photoinduced (PI) phase were taken with the fluorescence yield mode using a Lytle detector at BL9A. For the latter, a liquid He cryostat was employed to yield 11 K with high stability, and the sample, whose thickness is as thin as possible for the visible light (532 nm from a Nd:YAG laser) to penetrate, was kept irradiated during the XAFS measurements.

Results and discussion

Figure 1 shows the Co *K*-edge XANES. The spectral features and the edge energy positions clearly indicate that the HT [Fig. 1(a)] and LT [Fig. 1(b)] phases consist of hight-spin Co(II) and low-spin Co(II), respectively. This is consistent with the previous findings [2]. Upon irradiation at 11 K, the spectrum changes drastically [Fig. 1(c)] and becomes similar to the HT one. When the spectrum was simulated by summing 35% of the LT spectrum and 65% of the HT one, the experimentally obtained spectrum is actually well reproduced, as shown with the dashed line in Fig. 1(c). It is thus concluded that the PI phase is essentially identical to the HT phase of Co(II)HS. Since the spectrum of the Co(II)LS state should noticeably be dissimilar to that of Co(II)HS as is found in some Co(II) spin-crossover complexes, the possibility of Co(II)LS for the PI state is clearly excluded. After whole the XAFS measurements, the sample was once heated to 100 K and was subsequently cooled down again, the spectrum is converted completely to the LT phase [see Fig. 2(d)], this indicating no detectable radiation damages due to visible lights or X-rays.

The EXAFS spectra were analysed according to the conventional procedure. The obtained coordination numbers *N* and the interatomic distances *R* are as follows:
N=6.1±1.6 and *R*=2.081±0.021 Å for the HT phase,
N=6.1±1.1 and *R*=1.899±0.011 Å for the LT phase, and
N=4.6±2.2 and *R*=1.95±0.04 Å for the PI phases.
The PI phase provides an intermediate distance between the HT and LT phases.

In summary, it is revealed that the PI phase is essentially equivalent to the HT Co(II)HS phase. Upon irradiation, one electron in $DTBCat^{2-}$ is transferred to Co(III)LS, yielding Co(II)HS and $DTBSQ^{-}$ as

$$\text{LS-Co}^{(\text{III})}(\text{DTBSQ}^{-})(\text{DTBCat}^{2-})(\text{phen}) \xrightarrow{h\nu\ (532\,\text{nm})} \text{HS-Co}^{(\text{II})}(\text{DTBSQ}^{-})_2(\text{phen})\ .$$

References

[1] T.Yokoyama et al., Chem. Phys. Lett. **345**, 272 (2001).
[2] C.Roux et al., Inorg. Chem. **35**, 2846 (1996).
* yokoyama@ims.ac.jp

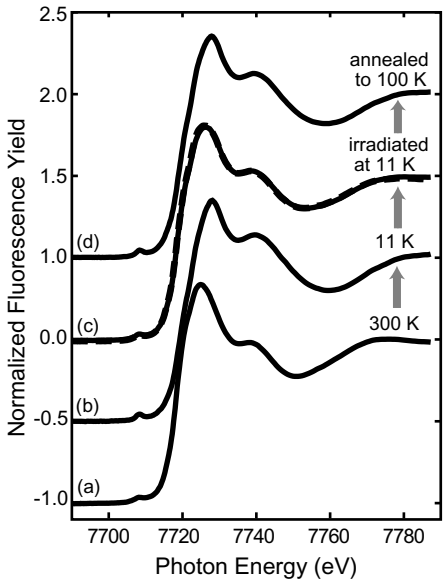

Fig. 1 Co *K*-edge XANES of (a) the HT phase, (b) the LT phase, (c) the PI phase and (d) the annealed phase after irradiation.

9A/2001G303

Local structure analysis of metal sulfide catalysts for HDS by means of in situ fluorescence X-ray absorption spectroscopy

Takeshi KUBOTA*[1], Naoto HOSOMI[1], Takashi MATSUI[2], Kyoko BANDO[2], Yasuaki OKAMOTO[1]
[1]Department of Material Science, Shimane-Univ., Matsue, Nishikawatsu, Shimane 690-8504, Japan
[2]National Institute of Advanced Industrial Science and Technology (AIST), Tukuba 305-8565, Japan

Introduction

Currently, Co-Mo sulfide catalysts are used for HDS treatment. It is well known that catalytic synergy generates between Co and Mo sulfides in the catalyst system. Numerous studies have been made to clarify the cause of the synergy effects by means of XAFS. But the information about active site of the Co-Mo catalysts is not enough under the reaction condition. The characterization of the catalyst during HDS reaction is necessary to clarify HDS mechanisms and catalyst improvement. In this study, we investigated the local structure analysis of supported Co-Mo sulfide catalysts under the sulfidation and thiophene HDS reaction conditions by means of in situ fluorescence XAFS.

Experimental

A continuous flow reaction line at atmospheric pressure was constructed in the beamline hatch at BL-9A. An in situ fluorescence XAFS cell was designed to have two windows for collection of incident and fluorescence X-ray. The reaction gas was treated by a post-catalyst, NaOH solution, ZnO column and combustor installed in the reaction line. The concentration of H_2S at outlet of the line was reduced upto less than 1ppm. The catalyst samples were pressed to self-supported disks. The disk was sulfided in a 5% of H_2S/H_2 gas (50ml/min) at 623 K. Then a 4% of thiophene/H_2 gas (50ml/min) was flowed to the sample at 623 K. Co K-edge XAFS spectra for Co-Mo catalysts were measured using a Lytle detector with a Fe filter. The synchrotron radiation was monochromatized by a Si(111) monochromator. CoS_x-MoS_2/Al_2O_3 and CoS_x-MoS_x/NaY catalysts were prepared by a CVD method using $Mo(CO)_6$ and $Co(CO)_3(NO)$.

Results and Discussion

Fig.1 shows Co K-edge XANES spectra for CoS_x-MoS_2/Al_2O_3 in a flow of H_2S/H_2 gas at room temperature. The spectrum measured in the air shows a sharp white line due to O_2 adsorption. But the peak intensity was immediately reduced by a flow of H_2S/H_2. Fig.2 shows Fourier transforms of k^3-weighted EXAFS oscillations of Co K-edge for Co-Mo sulfide catalysts measured at 623 K in the H_2S/H_2 flow, H_2 flow and HDS reaction. The difference in FT peak intensity is not observed between of calaysts measured in the H_2 flow and HDS reaction. It is considered that in the HDS reaction, Co atoms arehighly unsaturated.

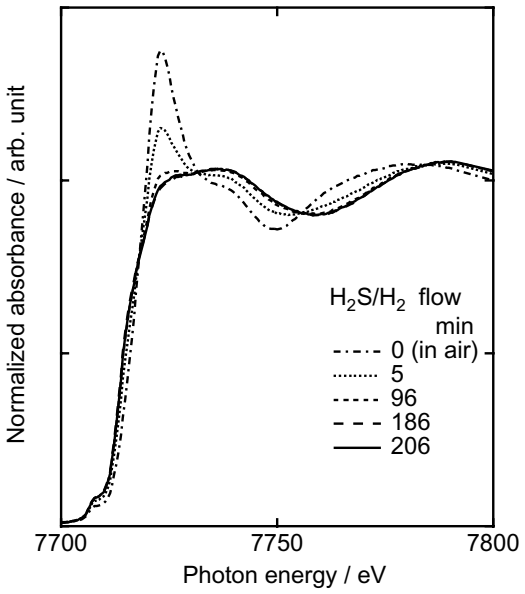

Fig. 1 Co K-edge XANES spectra for Co-Mo sulfide catalysts measured at room temperature in H_2S/H_2 flow.

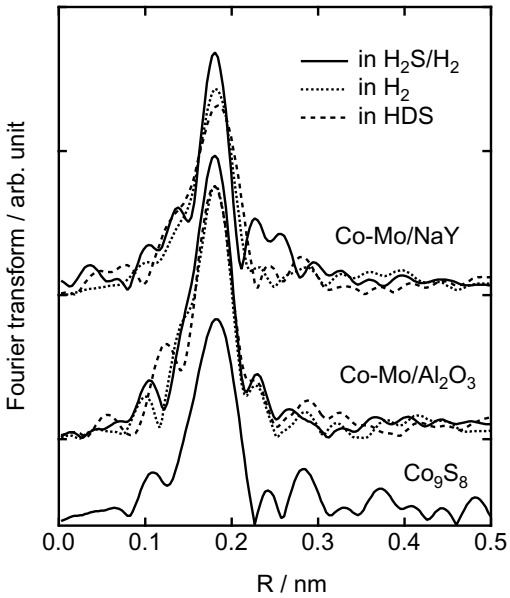

Fig. 2. Fourier transforms of k^3-weighted EXAFS oscillations of Co K-edge for Co-Mo sulfide catalysts measured at 673 K in the H_2S/H_2 flow, H_2 flow and HDS reaction.

*kubotake@riko.shimane-u.ac.jp

7C/2001G308

Structure of low concentrations of vanadium supported on titania determined by X-ray absorption fine structure combined with fluorescence spectrometry

Yasuo Izumi*[1], Fumitaka Kiyotaki[1], Ken-ichi Aika[1], Hideaki Yoshitake[2], Tae Sugihara[2], Takashi Tatsumi[2], Yasuhiro Tanizawa[3], Takafumi Shido[3], Yasuhiro Iwasawa[3]

[1] Interdisciplinary Graduate School of Science and Engineering, Tokyo Institute of Technology, 4259 Nagatsuta, Midori-ku, Yokohama 226-8502

[2] Graduate School of Environment and Information Sciences and Graduate School of Engineering, Yokohama National University, Tokiwadai, Hodogaya, Yokohama 240-8501

[3] Graduate School of Science, The University of Tokyo, Bunkyo-ku, Hongo 113-0033

Introduction

It is very difficult to measure XAFS data for low concentrations of V in the TiO_2 matrix. When 0.6 wt% of V is supported on TiO_2, XAFS measurements in transmission mode are difficult because the V K-edge jump is only 0.037 compared to a total absorption of 4. Experiments carried out in conventional fluorescence mode are also difficult because the photon number ratio of V Kα_1/Ti Kα_1 is only 0.012. When a solid-state detector (SSD; energy resolution ≈ 100 eV) is used, the V Kα_1 (4952.2 eV) peak can be separated from the Ti Kα_1 (4510.8 eV) peak. However, the Ti K$\beta_{1,3}$ (4931.8 eV) still overlaps the V Kα_1 peak. The ratio of V Kα_1/Ti K$\beta_{1,3}$ is 0.058. The selective detection of V K$\beta_{1,3}$ (5427.3 eV) is difficult using the SSD because scattered X-rays overlap. In this report, XAFS combined with a high-energy-resolution fluorescence spectrometer was applied to selectively monitor low concentrations of V on TiO_2.

Experimental section

The X-ray spectra were measured at 7C. A Si(111) monochromator was used and the beam was focused. The X-ray fluorescence from the sample was analyzed using a Rowland-type spectrometer (R = 180 mm) equipped with a Johansson-type Ge(331) crystal and a scintillation counter. The entire beam path was in helium, except for the I_0 ion chamber (N_2:He = 3:7). The V Kα_1 emission spectrum was measured with the excitation energy set at 5484.1 eV. Next, the V K-edge XANES was measured. The step scan was ≈0.25 eV. The dwell time of each data point was 60s, and two/three scans were measured for each sample. The energy position was reproduced within ±0.1 eV.

Results and discussion

Figure 1 shows the normalized V K-edge XANES spectra. In the case of conventional V/TiO_2, 3.0 (a) and 1.0 wt%-V (b), the rising edge appeared at 5480.8 – 5481.0 eV, corresponding to the valence state of +5. Two broad peak features were observed at 5489 and 5502 eV at nearly equivalent intensity. The two peak positions were similar to the case of $Mn_{1-x}V_{2-2x}Mo_{2x}O_6$($x$ = 0.10)(**1**) (d; 5490 and 5503 eV). The V site in **1** is coordinated by two terminal oxo ($d_{V=O}$ 1.661 – 1.693Å) and three farther oxygen atoms (d_{V-O} 1.913 – 2.151Å). The spectra (a) and (b) were also similar to XANES generated by FEFF 8.2 for a V site model A on anatase TiO_2(001) face (d_{V-O} 1.620 2, 1.922 2, and 2.151 Å) (e).

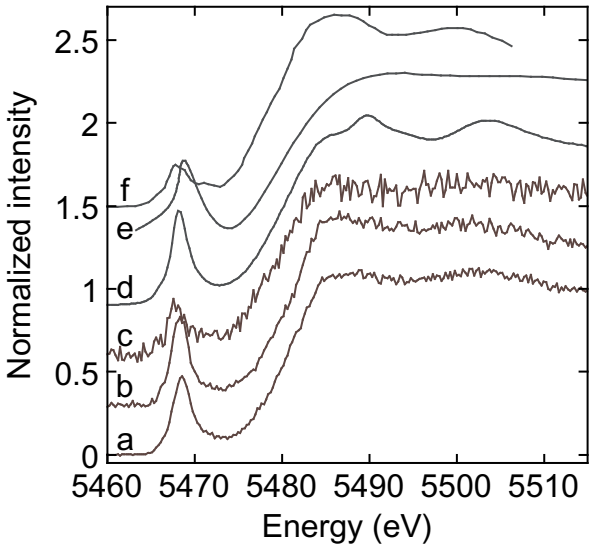

Figure 1. V K-edge XANES for V+TiO_2 catalysts measured using fluorescence spectrometry (a – c). V/TiO_2 of 3.0 (a) and 1.0 wt%-V (b). HSA V-TiO_2 (0.6 wt%-V, c). Reference XANES measured in transmission mode for $Mn_{0.9}V_{1.8}Mo_{0.2}O_6$ (d) and HSA TiO_2 (f). (e) was generated by FEFF 8.2 for vanadate model A on antase TiO_2(001).

For high-surface-area (HSA) V-TiO_2 prepared from V triisopropoxide oxide, Ti tetraisopropoxide, and dodecylamine, the rising edge position (5479.8 eV, c) was at lower energy than the case of V/TiO_2. Two broad peak features were observed at 5487 and 5505 eV. The post-edge pattern of V_2O_4 was relatively similar to (c), but the pre-edge position was at higher energy by 1.4 eV. The Ti K-edge data for HSA TiO_2 was compared to the V K-edge by shifting the energy by +499.8 eV (f). Both the post-edge pattern and pre-edge peaks were similar to the case of (c). A plausible structural model is that the V^{IV} sites are substituted on the Ti sites of HSA TiO_2.

*izumi@chemenv.titech.ac.jp

10B/2001G315

Structure of new rhodium catalysts prepared by surface molecular imprinting method

Mizuki Tada, Takehiko Sasaki, Takafumi Shido, and Yasuhiro Iwasawa
Graduate School of Science, the University of Tokyo
Hongo, Bunnkyo-ku, Tokyo 113-0033, Japan

Introduction

Surface molecular imprinting is a promising method to prepare molecular recognizing catalysts. Using this method, we have prepared a rhodium catalyst, which is active for olefin hydrogenation. The catalyst recognizes the fine difference of reactants and the activity is enhanced by forming silica over layers [1]. In this study, we have measured EXAFS to elucidate the reason for the ability of molecular recognition and the activity enhancement.

Experimental

Sample preparation: SiO_2 (Ox50, Degussa, preevacuated at 673 K, 1 h) was impregnated with a hexane solution of $Rh_2Cl_2(CO)_4$. Then excess $P(OCH_3)_3$ was added to the supported rhodium compound in diethyl ether followed by evacuation at 363 K for 3 h (Rh_{sup}). After that, $Si(OCH_3)_4$ and water vapors were condensed on the Rh_{sup} catalyst surface at room temperature followed by hydrolysis at 348 K for 7 h and evacuated at 363 K for 12 h to form SiO_2-matrix overlayers (Rh_{imp}).

EXAFS measurement and analysis: Rh K edge EXAFS for the Rh catalysts were recorded at BL-10B at 10-15 K with a transmission mode. After background subtraction, k^3 weighted EXAFS functions were Fourier transformed into a R-space and a curve fitting analysis was carried out in the R-space using the FEFFIT program [2]. The k and R ranges for the Fourier transformation and curve fitting were 30—140 nm^{-1} and 0.12—0.29 nm, respectively. Backscattering amplitudes and phase shifts were calculated by the FEFF8 code [3].

Result and discussions

Figure 1 (a) and (b) show FT of k^3 weighted EXAFS functions of Rh_{sup} and Rh_{imp}.. Table 1 shows the result of curve fitting analysis for Rh_{sup} and Rh_{imp}. After dosing $P(OCH_3)_3$, Rh—O and Rh—P bondings were observed at 0.203 and 0.224 nm with coordination numbers of 1.6 and 2.3. The result suggests that the Rh species after dosing of $P(OCH_3)_3$ were coordinated by two surface oxygen atoms and two $P(OCH_3)_3$ ligands. When the silica overlayer was deposited on the surface by a hydrolysis reaction of $Si(OMet)_4$, Rh—Rh bondings were formed and half of $P(OCH_3)_3$ was removed. The result suggests that the pore in which the Rh species exist shrank by the hydrolysis reaction and that the attached $(Rh(P(OCH_3)_3)_2O(s)_2)_2$ was pressed by the silica wall, which results in the formation of a Rh—Rh bonding and elimination of two $P(OCH_3)_3$ ligands. Thus, Rh_{imp} catalyst is Rh dimmer species coordinated by two surface oxygen atoms and a $P(OCH_3)_3$ ligand each. By exposing Rh_{imp} catalyst to hydrogen, Rh—Rh distance decreased to be 0.265 nm and when the catalyst after exposed to H_2 react with 3-methyl-2-pentene, the Rh—Rh distance increased reversibly to 0.270 nm. The result suggests that the hydrogenation reaction is associated by the cycle of shrinking and expansion of the Rh—Rh bond.

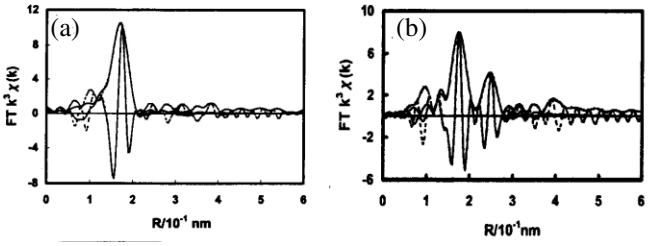

Figure 1. Fourier transformed EXAFS functions ($k^3\chi(k)$) for (a) Rh_{sup} and (b) Rh_{imp}.

Table 1. Structural parameters delivered by curve fitting analysis.

Sample/Shell	CN	R/nm	$\sigma^2/10^{-5}$ nm^2	ΔE_0/eV, Rf(%)
Rh_{sup}				
Rh-O	2(1)	0.203(3)	6(3)	6(4)
Rh-P	2(1)	0.224(5)	2(2)	0.2
Rh_{imp} (fresh)				
Rh-O	2.0(5)	0.211(2)	4(3)	11(2)
Rh-P	1.1(2)	0.221(1)	1(2)	1.4
Rh-Rh	1.3(3)	0.268(1)	7(1)	

References

[1] M. Tada, T. Sasaki, T. Shido, and Y. Iwasawa, *J. Phys. Chem. submitted.*
[2] E. A. Stern, M. Newville, B. Ravel, Y. Yacoby, Y. and D. Haskel, *Physica B* **208**, 117 (1995).
[3] A. L. Ankudinov, B. Ravel, J. J. Rehr, and S. D. Conradson, *Phys. Rev. B* **58**, 7565 (1998).

9C,10B/2001G316

In situ time-resolved energy-dispersive XAFS study on the structural changes of Rh/Al_2O_3 during CO adsorption and desorption

Akane SUZUKI[1], Aritomo YAMAGUCHI[2], Teiji CHIHARA[3], Yasuhiro INADA[4], Takafumi SHIDO[1], Kiyotaka ASAKURA[5], Masahiko Abe[2], Makoto Yuasa[2], Masaharu NOMURA[6] and Yasuhiro IWASAWA*[1]

[1]Graduate School of Science, The University of Tokyo, Tokyo 113-0033, Japan
[2]Faculty of Science and Technology, Tokyo University of Science, Chiba 278-8510, Japan
[3]The Institute of Physical and Chemical Research, Saitama 351-0198, Japan
[4]Research Center for Materials Science, Nagoya University, Nagoya 464-8602, Japan
[5]Catalysis Research Center, Hokkaido University, Sapporo 060-0811, Japan
[6]Institute of Materials Structure Science, Photon Factory, KEK, Ibaraki 305-0801, Japan

Introduction

Information on the structural change of metal clusters dispersed on oxide surfaces provides a clue to grasp the mechanism for catalyst reactions and dynamic processes at catalyst surface. The structure of Rh clusters in a highly dispersed $Rh/\gamma\text{-}Al_2O_3$ catalyst before and after CO adsorption has been studied by means of the conventional XAFS [1]. However, the conventional XAFS can not provide dynamic structural information on Rh clusters during CO adsorption and desorption. In this study, we tried to elucidate the structural change of $Rh/\gamma\text{-}Al_2O_3$ during the CO adsorption and desorption by means of time-resolved energy-dispersive XAFS (DXAFS).

Experimental

A 2wt% $Rh/\gamma\text{-}Al_2O_3$ catalyst was prepared by incipient wet impregnation of $\gamma\text{-}Al_2O_3$ (BET surface area: 150 m^2g^{-1}) with an aqueous solution of $RhCl_3 3H_2O$, followed by dry at 393 K for 30 h. Before CO adsorption, the dried catalyst was reduced at 613 K for 1.5 h under a flow of hydrogen and then evacuated at 573 K for 1 h.

DXAFS measurements were carried out at BL-9C in KEK-PF. A Si(311) bent crystal was used to focus polychromatic X-ray beam and a 1024-pixel position sensitive detector was used to record DXAFS spectra.

Results and Discussion

Figure 1 shows Fourier transformed k^3-weighted DXAFS functions for $Rh/\gamma\text{-}Al_2O_3$ during CO adsorption at 298 K. The spectra were measured every 0.8 s (0.4 s exposure time). The curve fitting analysis revealed that Rh-Rh bonds disappeared dramatically with an increase of the CNs of Rh-C and Rh-O (0-2.4 s). Then CN of Rh-CO and Rh-O increased slowly (7.2 s). Thus the structural transformation during the CO adsorption process proceeds through two steps. The present study demonstrates that the DXAFS technique is powerful and useful to monitor the dynamic structure change.

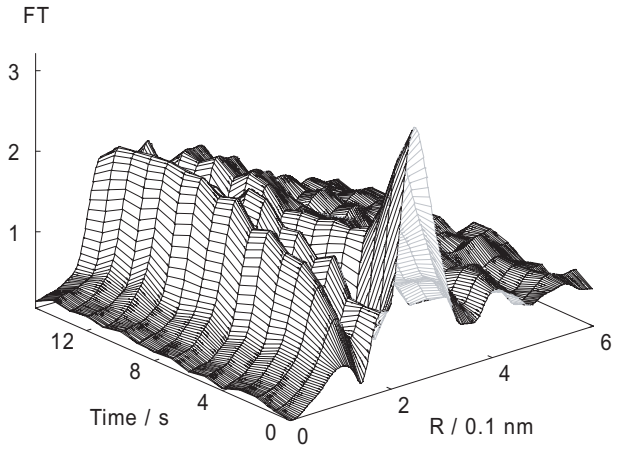

Figure 1. Fourier transformed k^3-weighted DXAFS functions for $Rh/\gamma\text{-}Al_2O_3$ during CO adsorption at 298 K

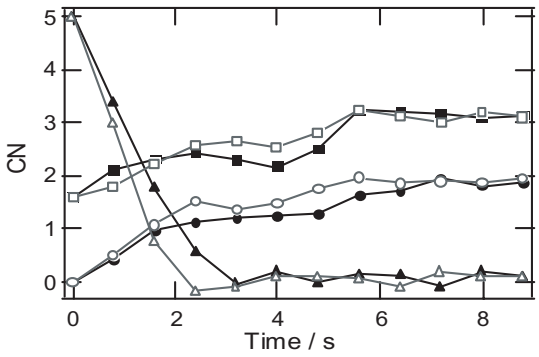

Figure 2. Change of coordination numbers (CN) of Rh-CO (○,●), Rh-Rh (△,▲) and Rh-O (□,■) during CO adsorption at 298 and 333 K .

[1] H. F. J. van't Blik et al., J. Am. Chem. Soc., **107**, 3139 (1985).

iwasawa@chem.s.u-tokyo.ac.jp

4A/2001P004

Chemical mapping of individual fluid inclusion by synchrotron X-ray fluorescence microprobe

Ken-ichiro HAYASHI*[1], Hiroki NAGASEKI[1], Atsuo IIDA[2]
[1]Graduate School of Science, Thoku Univ., Aoba-ku, Sendai 980-8578, Japan
[2]KEK-PF, Tsukuba, Ibaraki 305-0801, Japan

Introduction

Chemical composition of ore-forming fluid has fundamental importance to discuss the origin and evolution of ore-forming fluid, transport of ore-forming metals, and mechanism of ore mineral precipitation. Several substantial efforts have been made to develop the analytical techniques of individual fluid inclusions [1]. Among them, SXRF (synchrotron X-ray fluorescence microanalysis) requires special facility, and limited number of suitable microprobe beamlines is available (<10 sites worldwide). Applications of SXRF for the analysis of individual fluid inclusion have been previously reported by several researchers [2-7]. All these researches were carried out using synchrotron facilities in USA or UK. In this short report, we first present a preliminary result of SXRF analysis on fluid inclusion obtained by synchrotron source in Japan.

Samples

Doubly-polished thin section of quartz with thickness ~200 μm, commonly used in fluid inclusion study, was prepared in this study. Sample is from a prospect of porphyry copper deposit at Mocha, east of Iquique, northern Chile. Quartz specimen contains large amount of fluid inclusions. They are grouped into 2-phase type, vapor containing liquid inclusion, and polyphase type, solid(s) containing vapor and liquid inclusion. Distribution pattern of inclusions in quartz suggests that polyphase inclusions are primary in origin. Daughter mineral observed in the polyphase inclusions is NaCl, and most polyphase inclusion contains unknown opaque mineral besides NaCl.

Results of heating experiments of polyphase inclusions are summarized as follows. The bubble disappeared at variable temperatures of 254°-351°C (n = 17) and NaCl crystal dissolved at 261°-387°C (n = 16). The NaCl crystal dissolved after the disappearance of bubble in all cases. The NaCl equivalent salinity calculated from the dissolution temperatures of the halite daughter salt varies between 35.1 and 45.7 %. No significant change was observed on opaque daughter mineral during heating up to 500°C.

Results

The XRF spectrum obtained from a polyphase fluid inclusion that locates ~20 μm depth beneath the surface of quartz reveals the presence of Si, Ca, Ti, Mn, Fe, Ni, Cu, Zn, As, and Br. The background of XRF spectrum was obtained from quartz of fluid inclusion free portion just beside the fluid inclusion analyzed. In addition to silicon, Ti and Ni were detected from host quartz crystal. The fluid inclusion contains elements such as Mn, Fe, Cu, Zn, As and Br. However, many other elements such as Na and Cl are also likely to be present, but were not detected owing to limitations in detector sensitivities coupled with signal loss by absorption of X-rays in the host quartz crystal. In the case where inclusion was located <5 μm from the surface of quartz, small signal generated by Cl was observed. However, SXRF analysis is not an adequate method to analyze light elements especially mass number <Ca [6]. In contrast with this, heavy elements are very sensitive to SXRF. Although bromine content in fluid inclusion is usually much less than that of Cl, it is clearly detected from hypersaline inclusion.

We have succeeded to map the distribution of several elements in single fluid inclusion. During the accumulation of SXRF data, specimen was moved every 2 μm by X-Y stage; images were then composed from a total of 400 point analyses. The map suggests elements except As distribute homogeneously in liquid phase of fluid inclusion. Although this fluid inclusion contains daughter crystal of NaCl, concentrations of Br, Fe, Mn and Zn are not obviously high in solid phase. However, concentration of arsenic in daughter crystal probably in opaque mineral is higher than that in liquid phase. Since effect of absorption of X-ray by host quartz was not known in this stage, quantitative concentrations of elements in the fluid inclusion are unclear. However, SXRF is the powerful tool for research of ore deposits.

References

[1] T. J. Shepherd and A. H. Rankin, Rev. Econ. Geol., 10, 125 (1998).
[2] J. D. Franz et al., Chem. Geol., 69, 235 (1988).
[3] A. J. Anderson et al., Canada. Mineral., 33, 499 (1995)
[4] J. A. Mavrogenes et al., Geochim. Cosmochim. Acta, 59, 3987 (1995)
[5] A. H. Rankin et al., Geochim. Cosmochim. Acta, 56, 67 (1992)
[6] D. A. Vanko et al., Chem. Geol., 7, 251 (1998)
[7] D. A. Vanko and J. A. Mavrogenes, Rev. Econ. Geol., 7, 251 (1998)

* khayashi@mail.cc.tohoku.ac.jp

8A, 13C/2001P005

Carbon *K*-edge NEXAFS study of carbonaceous matter in the Allende (CV3) carbonaceous chondrite

Fumio KITAJIMA[*1], Kazuhiko MASE[2], Tomoki NAKAMURA[1], Eiichi KOBAYASHI[2], Kouji ISARI[3], and Yoshinori KITAJIMA[2]

[1]Kyushu University, Hakozaki, Fukuoka 812-8581, Japan.
[2]KEK-PF, Tsukuba, Ibaraki 305-0801, Japan.
[3]Hiroshima University, Kagamiyama, Higashi-hiroshima 739-8526, Japan.

Introduction

Various techniques, such as X-ray diffraction, Raman spectroscopy, and pyrolysis gas chromatography, have been applied to the characterization of the carbonaceous matter in carbonaceous chondrites. The major fraction of this matter is solvent insoluble macromolecular matter. Recently, some researchers have begun to use XANES spectra for the characterization of some extraterrestrial carbonaceous materials [1, 2, 3].

In this investigation, we tried to apply the XANES technique to the evaluation of the degree of graphitization of the carbonaceous matter, and the thermal history of its parent bodies.

Experimental

The Allende carbonaceous chondrite (CV3; Carbon *ca.* 0.3 %) was powdered and pressed on the copper plate (10mm × 10mm × 1mm). This chondrite has been moderately heated in its parent body [4]. A commercial highly oriented pyrolytic graphite (HOPG) crystal was used as a standard. Carbon *K*-shell excitation spectra were observed at the beamline BL-13C.

Results and Discussion

The XANES spectra of HOPG (Figs. 1a, b) were observed satisfactorily, showing dependence on angle of X-ray incidence, and the spectrum of Allende (Fig. 1c) shows a strong C=C π* resonance at 285 eV, which is characteristic of aromatic carbon, in accord with the previous reports on some extraterrestrial carbonaceous materials [1, 2, 3]. In the case of Allende, the spectrum does not depend on angle of X-ray incidence.

However, the absorbtion intensity of the resonance at 285 eV is stronger than that of above the carbon edge, which reflects the total carbon number density. Cody III et al. (1999) reported that in the case of Murchison (CM2), the intensity above the carbon edge was comparable to that of the 285-eV feature [1]. These suggest that the size of carbonaceous matter in Allende is smaller than that in Murchison, although Allende is a moderately heated chondrite and the size of its carbonaceous matter should be expected to be larger than that of Murchison. The reason of this disagreement remains unclear.

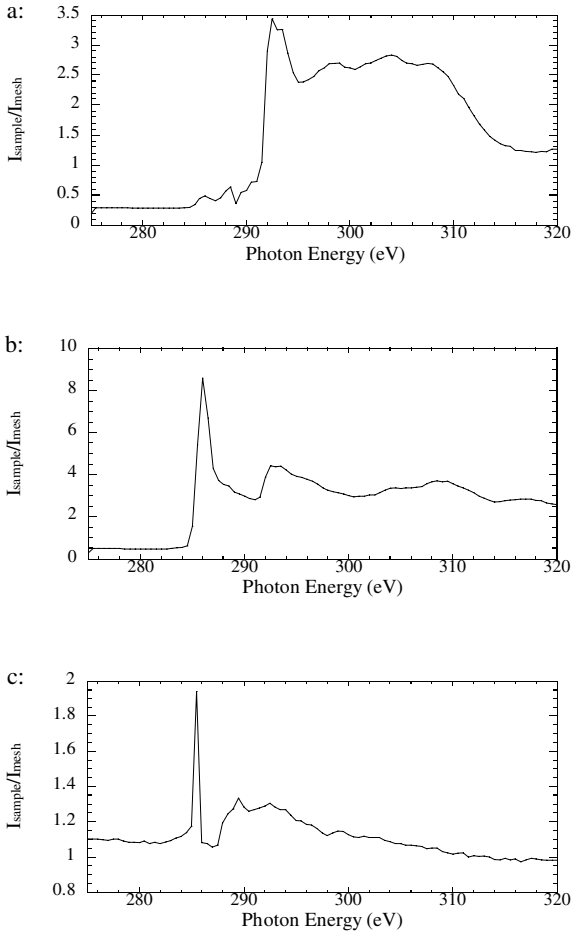

Fig 1. Carbon *K*-edge XANES spectra
a: HOPG $\theta = 90°$, b: HOPG $\theta = 30°$, c: Allende
θ = angle of X-ray incidence

References

[1] G. D. Cody III et al., *Meteorit. Planet. Sci.* **34**, Suppl., A25-A26 (1999).
[2] S. Derenne et al., *Meteorit. Planet. Sci.* **36**, Suppl., A49 (2001).
[3] L. P. Keller et al., *Meteorit. Planet. Sci.* **35**, Suppl., A86 (2000).
[4] F. Kitajima et al., *Geochim. Cosmochim. Acta* **66**, 163-172 (2002).

*kitajima@geo.kyushu-u.ac.jp